Journal of Environmental Chemical Engineering 13 (2025) 115781

Contents lists available at ScienceDirect

Journal of Environmental Chemical Engineering

journal homepage: www.elsevier.com/locate/jece

Harnessing MOF-based and derived catalysts for efficient BTEX oxidation: Progress, challenges, and future directions

David Murindababisha [a,b,1], Zongshuang Wang [c,1], Zhiyu Xiao [a], Abubakar Yusuf [a], George Zheng Chen [d], Jianrong Li [e,*], Jun He [a,f,**]

[a] Department of Chemical and Environmental Engineering, University of Nottingham Ningbo China, Ningbo 315100, China
[b] Department of Mechanical Engineering, Tumba College, Rwanda Polytechnic, P.O. Box 6638, Rulindo, Rwanda
[c] Chinese Research Academy of Environmental Sciences, Beijing 100085, China
[d] Department of Chemical and Environmental Engineering, Faculty of Engineering, University of Nottingham, Nottingham NG7 2RD, UK
[e] Institute of Urban Environment, Chinese Academy of Sciences, Xiamen 361021, China
[f] Nottingham Ningbo China Beacons of Excellence Research and Innovation Institute, Ningbo 355101, China

ARTICLE INFO

Keywords:
MOF-derived oxides
BTEX
Monometallic MOFs
Bimetallic MOFs
Noble metals
Transition metals

ABSTRACT

Metal-organic framework (MOF)-derived catalysts have emerged as promising materials for the catalytic oxidation of BTEX (benzene, toluene, ethylbenzene, and xylene) pollutants due to their high surface area, customizable pore structures, and uniform metal dispersion. This review critically examines recent advancements in MOF-based and MOF-derived catalysts for BTEX oxidation, emphasizing their structural and compositional innovations. The analysis categorizes catalysts into noble metal-supported, single transition metal oxide, and bimetallic oxide catalysts, quantitatively comparing their catalytic performance, including conversion efficiency, selectivity, and stability under varying conditions. Notably, noble metal-supported catalysts achieve BTEX conversions exceeding 90 % at temperatures as low as 180 °C, while bimetallic oxides reveal enhanced durability and resistance to deactivation. This review also provides a mechanistic perspective on catalytic degradation pathways, including Mars-Van Krevelen, Langmuir-Hinshelwood, and Eley-Rideal models, highlighting the role of MOF-derived nanostructures in facilitating oxygen vacancy formation and active site exposure. Addressing key challenges such as catalyst deactivation due to SO_2 poisoning and water vapor, we propose innovative strategies for catalyst regeneration and enhanced longevity. This work fills a crucial gap in MOF-based catalytic research by systematically correlating structural properties with catalytic efficiency, offering a roadmap for future advancements in sustainable air pollution control.

1. Introduction

Benzene, toluene, ethylbenzene, and xylenes (*para, meta,* and *ortho*-xylene) commonly known as BTEX (Fig. 1) are volatile organic compounds (VOCs) originating from petroleum oil and its derivatives, such as coal, wood tars, and gasoline [1–4]. Despite their widespread industrial use, their volatility and toxicity pose significant health risks including impact on the blood, immune, and central nervous systems [5,6], and severe conditions like liver and kidney damage or coma [7]. Regulatory bodies like the Environmental Protection Agency (EPA) and the Occupational Safety and Health Agency have set limits on BTEX levels in air and water to mitigate health risks [4,8,9]. Moreover, BTEX are primary pollutants categorized by the USEPA and potential human carcinogens designated by the International Agency for Research on

Abbreviations: 1D, One dimensional; 2D, Two dimensional; 3D, Three dimensional; BDC, Benzenedicarboxylic acid; BTC, Benzene-1,3,5-tricarboxylate; BTX, Benzene, Toluene and Xylenes; DMF, N, N-dimethylformamide; EDTA, Ethylene diamine tetraacetic acid; DRIFS, Diffuse reflectance, infrared Fourier transform spectroscopy; MIL, Matérial Institut Lavoisier; MOFs, Metal-organic frameworks; NPs, Nanoparticles; PBA, Prussian blue analogue; ppb, Parts per billion; ppm, Parts per million; SV, Space velocity; TPD, Temperature-programmed desorption; TPSR, Temperature-programmed surface reaction; UiO-66, Universitetet i Oslo-66; US, United States; WHSV, Weight hourly space velocity; ZIF, Zeolitic imidazole framework.

* Corresponding author.
** Corresponding author at: Department of Chemical and Environmental Engineering, University of Nottingham Ningbo China, Ningbo 315100, China.
E-mail addresses: jrli@iue.ac.cn (J. Li), jun.he@nottingham.edu.cn (J. He).
[1] These authors contributed equally to this work.

https://doi.org/10.1016/j.jece.2025.115781
Received 12 September 2024; Received in revised form 5 February 2025; Accepted 12 February 2025
Available online 14 February 2025
2213-3437/© 2025 The Authors. Published by Elsevier Ltd. This is an open access article under the CC BY-NC license (http://creativecommons.org/licenses/by-nc/4.0/).

Cancer [1,2,7,10]. Beyond health concerns, BTEX contribute to environmental harm by contributing to photochemical smog, climate change, and ozone depletion [9,11–14]. Due to their significant impact on both human health and the environment [9,15], there is an urgent need for efficient technologies to control BTEX emissions from polluted gas streams to improve air quality and safeguard human health.

Current techniques face limitations in efficiency, stability, and cost-effectiveness under various conditions. MOF-based catalysts offer promising solutions due to their tunable porosity, large surface area, and catalytic potential. Key challenges for MOF-based catalyst development include improving stability and resistance to contaminants like SO_2 and H_2O vapors, optimizing performance across diverse operating environments, and addressing deactivation issues. Advances in these areas could enable more robust and sustainable BTEX control, contributing to both regulatory compliance and enhanced public health.

Various technologies are available for reducing BTEX emissions, encompassing non-destructive methods such as absorption [16], adsorption [17], condensation [18], and membrane separation [19]; and destructive methods including thermal incineration [20], non–thermal plasma [21], catalytic oxidation [22], and photocatalysis [23]. Economically viable, non-destructive techniques are recognized for their ability to recover BTEX. However, adsorption and condensation face limitations due to their elevated processing and maintenance expenses, and membrane separation is not widely endorsed in the industry owing to its lower membrane flux [24–26].

Within the destructive methodologies summarized in Fig. 2, the non-thermal plasma approach stands out as it can transform BTEX into harmless end products at room temperatures, requiring lower consumption of energy and presenting fewer demands on the operating environment. Nonetheless, it is worth noting that this technique is often characterized by CO_2 selectivity [27]. Photocatalytic technology shows promise in effectively eliminating BTEX contaminants at lower concentrations due to its advantageous characteristics, including minimal energy consumption, efficacy against a range of contaminants, and environmentally friendly end-products [28]. However, the production of harmful by-products is unavoidable in many instances, and factors like the concentration of pollutants and the control of irradiation of light also impact the application of photocatalytic technology [29]. Traditional thermal incineration can transform BTEX into benign CO_2 and H_2O, but this process entails substantial energy consumption [30]. On the contrary, catalytic oxidation appears more promising because of its high efficiency, selectivity of eco-friendly products, and lower operational temperatures [31]. The main focus of this technique revolves around creating catalysts that are both effective and economical. Two primary categories of catalysts, namely non-noble metal and noble metal catalysts, have been extensively researched [32–34]. Moreover, the catalysts' performance is primarily influenced by their physicochemical attributes, including metal valence, specific surface area, oxygen vacancies, and reactive oxygen species. The catalyst morphology further impacts the active site distribution, consequently influencing catalytic activity [35]. Hence, designing an appropriate structure can significantly improve the catalytic characteristics [36].

Metal-organic frameworks (MOFs) represent an innovative class of porous materials, existing in 1D (one-dimensional), 2D (two-dimensional), or 3D (three-dimensional) structures. They are created through the self-assembly of clusters or metal ions as connecting elements and organic linkers as support, gaining considerable interest for diverse applications in multiphase catalysis [37,38]. MOFs own a clear superiority over conventional mesoporous materials like zeolites and activated carbon because of their repetitive, well-organized crystal structure, and substantial specific surface area [38,39]. The final application of MOFs is influenced by the morphology of the structure and physicochemical properties (including surface functionality, pore size, and surface area), which can be adjusted by selecting various experimental methods. In this scenario, MOFs can serve as a sacrificial template for producing porous nanomaterials [39].

Elevated pyrolysis temperature can eliminate the non-stable linker and transform the MOF into a durable metal oxide. The clusters and metal ions, arranged in a periodic manner within MOFs, can undergo conversion into nanoparticle metals and exhibit uniform distribution in the resultant composite [40]. Derivatives of MOFs can attain supplementary characteristics beyond the inherent higher specific surface area, porous structure, and original fundamental MOF morphology, including enhanced properties such as resistance to water [41,42]. Pyrolysis conditions substantially impact the physicochemical properties and hence the performance of MOF-derived catalysts. For instance, under high temperatures, the Zn in ZIF-8 undergoes evaporation and generate more pores which facilitated in the improvement of material performance [43,44]. Nanostructured materials produced through the treatment of suitable MOFs have found recent applications in various domains, including catalysis, adsorption, storage of gaseous fuels, supercapacitors, and chemical hydrogen storage [45–47] The significance of catalysts' structural properties for BTEX oxidation entails the need to carefully choose precursors and apply suitable treatment conditions when preparing MOF-derived catalysts to ensure high efficiency.

Recently, there has been a growing research interest on MOF-derivatives catalysts for BTEX emission control as shown in Fig. 3. These derivatives could retain the elevated specific surface area characteristic of the original MOF, facilitating the exposure of additional active sites. The uniform structure also aids in effective pollutant diffusion. Additionally, the presence of numerous electron-deficient open metal sites enhances the interaction with BTEX as active sites [38]. These attributes significantly enhance its efficacy in combating BTEX. According to findings in the literature, the existing techniques for

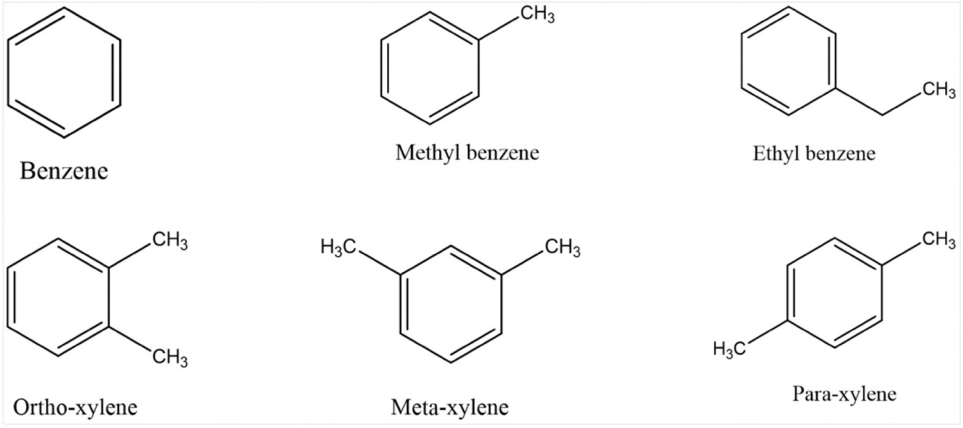

Fig. 1. Chemical structures of BTEX compounds.

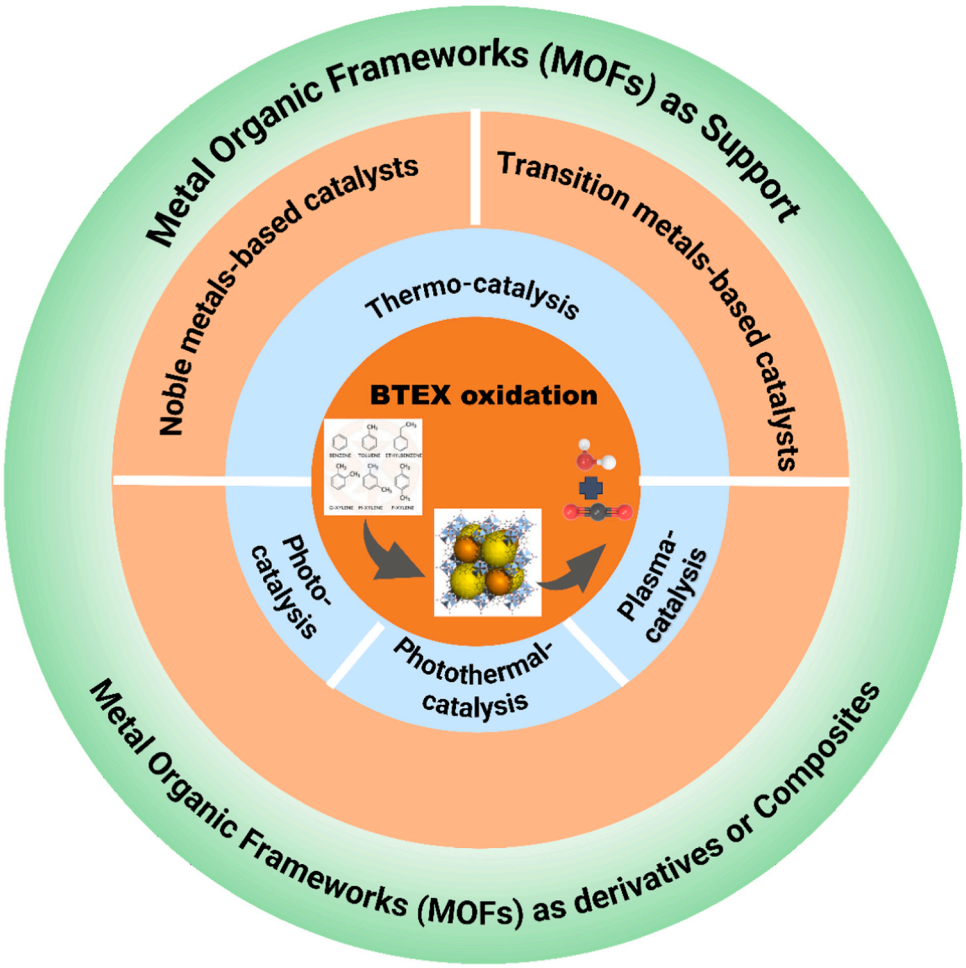

Fig. 2. Schematic picture of MOF and MOF-derivatives in BTEX catalytic oxidation.

producing MOF derivatives involve pre-assembly methods such as aliovalent substitution and post-modification approaches like creating core-shell structures, introducing other metals, liquid phase reduction, grinding, and more. The distinct preparation and combination methods applied in the production of MOF derivatives have resulted in a diverse array of experimental outcomes in BTEX catalytic oxidation [37,39].

In recent times, numerous reviews have explored nanomaterials derived or supported by MOFs and their diverse applications in various fields [37–40]. On the other side, various reviews on BTEX elimination have been presented and the recent one was reported by Vellingiri et al. where they focused on sorptive removal of BTEX from water and wastewaters [48]. Nonetheless, there is a noticeable absence of a comprehensive review on MOFs-derived catalysts specifically focused on the oxidation of BTEX compounds. This review aims to fill the gap by compiling and analyzing recent advancements in this area. The existing literature provides a wide range of experimental outcomes due to the diverse preparation methods and precursor types used in the production of MOF-derived materials. However, there is a need for a detailed comparison and analysis of these methods to determine their effectiveness under various operational conditions and contaminant concentrations. Therefore, this review delves into research outcomes concerning BTEX catalysis involving various preparation methods and precursor types considering diverse operational conditions and contaminant concentrations (Tables 1 and 2). Besides, the impact of SO_2 and water vapor on the deactivation of MOF-based/derived catalysts is an area that requires further exploration. Thus, this review intends to address this by examining the mechanisms involved in the degradation of BTEX over various MOF-derived catalysts in the presence of these deactivating agents. Furthermore, there is a need for a deeper understanding of the mechanisms through which BTEX compounds are degraded over MOF-based/derived catalysts. This review presents and discusses these mechanisms, providing insights that could lead to the development of more effective catalysts. The conclusion provides insights into future development trends and highlights challenges in the current application of this technology. Although current studies have made significant progress, there are still challenges and limitations in the application of MOF-based/derived catalysts for BTEX degradation. This review highlights these challenges and provide insights into potential future development trends to overcome these obstacles and improve the technology.

2. Characterization methods of MOF-based catalysts

To assess the structural, chemical, thermal and catalytic properties of MOF-based catalysts, characterization techniques are essential. Common methods which are mostly used include X-ray diffraction (XRD) used to determine the crystalline structure, crystallinity and phase purity of MOFs and MOF-derived catalysts; Scanning Electron Microscope (SEM) used to offer detailed images of the surface morphology and particle size; Transition Electron Microscope (TEM) used to provide high-resolution images to observe internal structure and dispersion of metals on the MOF; Energy-Disperse X-ray Spectroscopy (EDX or EDS) used to confirm the presence of specific elements within the MOF; X-ray Photoelectron Spectroscopy (XPS) used for the analysis of surface composition and oxidation states of elements which facilitate to evaluate surface chemistry, oxidation states changes, and interaction

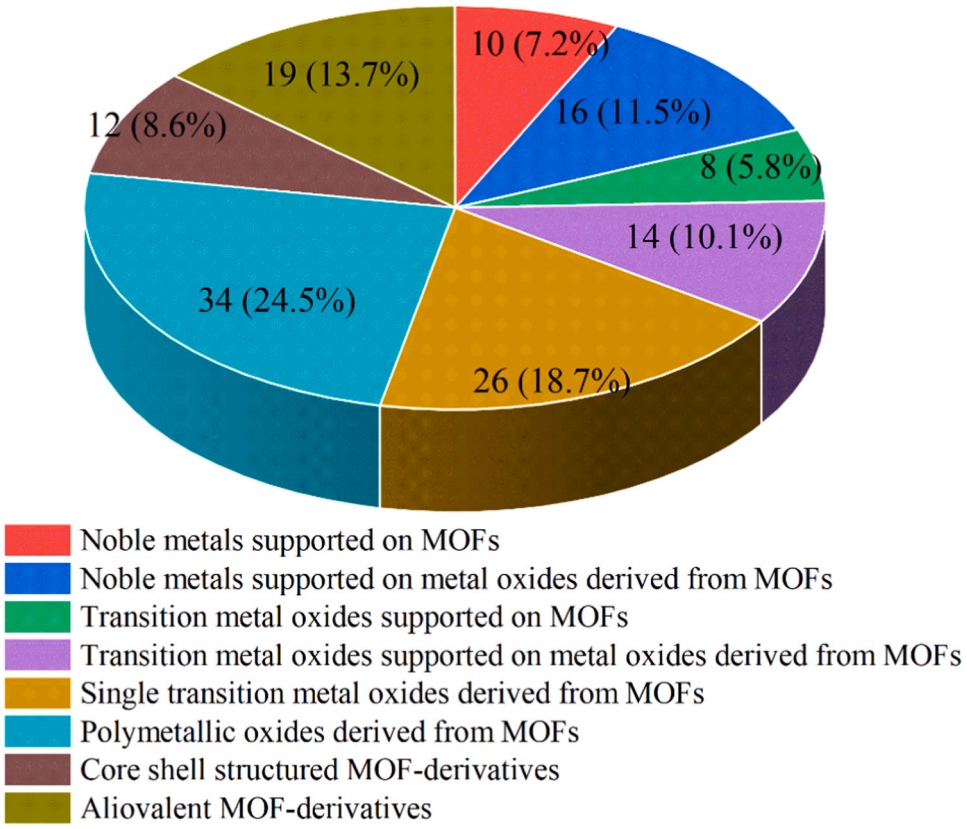

Fig. 3. Various types of analyzed MOF-based catalysts for BTEX oxidation.

Table 1
Properties and working conditions summary of MOF-derived noble metal catalysts for BTEX oxidation.

Catalyst	Parent MOF	Preparation technique	BTEX compound	Catalyst amount (g)	Concentration (ppm)	WHSV (mL/(g.h))	T_{90} (°C)	Ref
Pt/UiO−66	UiO−66	Incipient wetness impregnation	Toluene	0.1	1000	40,000	249	[78]
Ag-U	UiO−66	Liquid phase reduction	Toluene	0.1	1000	30,000	300	[75]
Pd-U-EG	UiO−66	Ethylene glycol reduction	Toluene	0.1	1000	30,000	198	[59]
Pd/UiO−66	UiO−66	Conventional wetness impregnation	Toluene	0.075	1000	120,000	260	[76]
Ag-Ce-BTC	Ce-BTC	One pot synthesis	Toluene	0.1	1000	30,000	226	[63]
Pt/CoO_x	ZIF−67	Pyrolysis and glycol reduction	Toluene	0.2	1000	30,000	177	[79]
Pd@ZrO_2	UiO−66	Calcination	BTX	0.1	1000	30,000	218	[80]
Pd/Mn_3Ce_2	Mn/Ce-BTC	Pyrolysis	BTX	0.1	1000	40,000	185	[57]
Pd/Mn_3Ce_2	Mn/Ce-MOF	Pyrolysis	Toluene	0.1	1000	30,000	190	[66]
Pt/MOF-BTC	Ce-MOF	Hydrothermal and solvothermal with $NaBH_4$ reduction	Toluene	0.1	1000	30,000	149	[64]
Pt/MOF−800	MOF−800	Hydrothermal and solvothermal with $NaBH_4$ reduction	Toluene	0.1	1000	30,000	178	[64]
Pt/UiO−66	UiO−66	Hydrothermal and solvothermal with $NaBH_4$ reduction	Toluene	0.1	1000	30,000	193	[64]
Pt/$MnCoO_x$	MnCo-MOF	Self-assembly	Toluene	0.1	1000	48,000	275	[81]
Pt@M-Cr_2O_3)	MIL−101-Cr	Impregnation and pyrolysis	Toluene	0.2	1000	20,000	144	[82]
Pd–UiO−66-M	UiO−66	Ethylene glycol reduction	Toluene	0.1	1000	30,000	200	[83]
Pt@Co_3O_4	ZIF−67	In situ growth and calcination	Toluene	0.2	1000	60,000	179	[72]
Pd/ Co_3O_4	ZIF−67	Pyrolysis	Benzene	0.1	100	60,000	221	[71]
Pt/UiO−66	UiO−66	Impregnation-reduction	Toluene	0.02	500	60,000	180	[60]
Ru/Co_3O_4-MOF	ZIF−67	Pyrolysis	Toluene	0.1	1000	60,000	238	[70]
Pd@ZrO_2	Pd@UiO−66	Pyrolysis	Toluene	0.1	1000	30,000	218	[58]
Pd/UiO−66 (Ce)	UiO−66(Ce)	Reduction	o-xylene Toluene Benzene	0.1	1000	30,000	192 209 228	[84]

between MOF ligands and metal ions; Fourier Transform Infrared Spectroscopy (FTIR) for identifying functional groups and chemical bonds within the MOF framework to confirm organic linkers in MOF, check for structural integrity, and detect changes in bonding post-catalysis; Brunauer-Emmet-Teller (BET) surface area analysis for measuring surface area, pore volume, and pore size distribution; Thermogravimetric Analysis (TGA) for measuring thermal stability and decomposition patterns; Inductively Coupled Plasma (ICP) analysis used

Table 2
Properties and working conditions summary of MOF-derived transition metal oxide catalysts for BTEX oxidation.

Catalyst	Parent MOF	Preparation technique	BTEX compound	Catalyst amount (g)	Concentration (ppm)	WHSV (mL/(g.h))	T_{90} (°C)	Ref
Co_3O_4	Co-MOF	Precipitation	Toluene	0.2	1000	20,000	239	[106]
Co_3O_4	Co-MOF−74	Precipitation	Toluene	0.2	1000	20,000	239	[107]
Mn-MIL−100	Mn-MIL−100	Precipitation	Toluene	0.1	1000	30,000	183	[112]
CeO_2	Ce-UiO−66	Precipitation	Benzene	0.6	1000	22,500	225	[98]
CeO_2	Ce-UiO−66	Precipitation	Toluene	0.6	1000	22,500	206	[98]
CeO_2	Ce-UiO−66	Precipitation	Xylene	0.6	1000	22,500	250	[98]
Co_3O_4	Co-ZIF−67	Precipitation	Toluene	0.6	12,000	21,000	259	[150]
Mn_3O_4	Mn-MOF−74	Precipitation	Toluene	0.05	1000	20,000	218	[103]
CeO_2	Ce-MOF	Precipitation	*o*-xylene	0.1	200	120,000	195	[151]
CeO_2	Ce-MOF	Hydrothermal	*o*-xylene	0.16	500	48,000	198	[152]
Mn_2O_3	Mn-MIL−100	Precipitation	Toluene	0.1	1000	30,000	262	[153]
CeO_2	Ce-MOF−808	Precipitation	Toluene	0.1	1000	60,000	278	[154]
CeO_2	Ce-BTC	Precipitation	*o*-xylene	0.16	500	48,000	193	[155]
CeO_2	Ce-BDC	Precipitation	Toluene	0.1	1000	20,000	223	[156]
FeO_x	Fe-MOF	Precipitation	Toluene	0.3	500	20,000	249	[157]
$Co_2Cu_1O_x$	CoCu-MOF−74	Grinding	Toluene	0.1	1000	30,000	220	[99]
$Co1Mn1O_x$	Mn/Co-MOF	Impregnation	Toluene	0.1	1000	20,000	227	[115]
UiO−66-CeCu	UiO−66-Ce	Coprecipitation	Toluene	0.1	1000	30,000	223	[144]
MnO_x@ZrO_2	Mn@MOF−808-Zr	Impregnation	Toluene	0.1	1000	60,000	260	[117]
Cu-CoO_x/C	Co/Cu-BTC	Impregnation	Toluene	0.3	1000	40,000	243	[158]
CeO_2-MnO_x	Ce/Mn-BTC	Impregnation	Toluene	0.2	1000	48,000	277	[159]
$CoCeO_x$	CoCe-BDC	Solvothermal	Toluene	0.1	500	34,500	227	[160]
MnO_x-CeO_2	Ce-Mn-MOF−74	Coprecipitation	Toluene	0.05	1000	60,000	220	[161]
Sm/CeO_2	Sm/Ce-MOF	Coprecipitation	Toluene	0.05	1000	60,000	211	[142]
$CeCuO_x$	CeCu-BDC	Coprecipitation	Toluene	0.15	500	23,000	186	[162]
$CuMnO_x$	CuMn-MOF	Escape-by-craft	Toluene	0.1	1000	60,000	208	[163]
$MnCeO_x$	MnCe-BTC	Hydrothermal	Toluene	01	1000	30,000	244	[146]
MnO_x/Co_3O_4	Mn/ZIF−67-Co	Impregnation	Toluene	0.025	1000	120,000	242	[116]
MnO_x/Cr_2O_3	Mn/MIL−101-Cr	Impregnation	Toluene	0.1	1000	20,000	269	[100]
$CoMn_xO_x$	Mn/ZIF−67-Co	Oxidation-etching	Toluene	0.05	1000	60,000	219	[118]
$CoCu_1O_x$	Cu/Co-MOF	Impregnation	Toluene	0.1	1000	20,000	208	[125]
Co−Fe-δ-MnO_2	Co-Fe-PBA	Coprecipitation	Toluene	0.1	1000	30,000	225	[164]
Cu-CeO_x	Cu/CeO_x-MOF−808	EDTA grafting	Toluene	0.1	1000	60,000	226	[124]
$MnCeO_\delta$/Co_3O_4	$MnCeO_\delta$ /Co_3O_4-NC	Impregnation	Toluene	0.5	1000	40,000	227	[165]
$CeCoO_x$	Ce[$Co(CN)_6$]	Hydrothermal	Toluene	0.4	3000	30,000	168	[122]
$CeCoO_x$	CeCo-MOFs-MNS	Precipitation and Impregnation	Benzene Toluene δ-xylene	0.4	3000	30,000	204 249 288	[166]
CoCeOx	Ce-BTC	Impregnation	Toluene	0.15	1000	120,000	262	[167]
$CuCoO_x$	CuCo-ZIF	Pyrolysis	Toluene benzene ethylbenzene o-xylene	0.15	1000	40,000	209 201 223 248	[168]
$MnFeO_x$	MnFe-MOF−74	Pyrolysis	Toluene	0.15	1000	40,000	262	[169]
$Ce_aMn_{3-a}O_4$	MnCe-MOF−74	Pyrolysis	Toluene	0.3	1000	20,000	214	[170]
La/CoO_x	Co-MOFs	Impregnation and calcination	Toluene	0.1	1000	60,000	227	[171]
$LaMO_3$	LMO-MOF	Solvo-thermal	Toluene	0.1	1000	60,000	278	[172]
$CeCo_aO_x$	Ce-MOF	Pyrolysis	Toluene	0.15	1000	40,000	226	[173]
$CuCoO_x$	CuCo-ZIF	Pyrolysis	Toluene	0.15	1000	40,000	209	[174]
$CuCoO_x$	Co-MOF−74	Pyrolysis	Toluene	0.2	1000	36,000	212	[175]
2Mn1Co	Co-MOF	Pyrolysis	Toluene	0.1	1000	30.000	245	[176]
$MnCeO_x$/ cordierite	MnCe-BDC	Hydrothermal and pyrolysis	o-xylene	0.05	1000	10,000	283	[177]

to quantify metal content within the MOF; UV-Visible Diffuse Refractance Spectroscopy (UV-Vis DRS) for investigating the electronic properties and band gaps particularly in photocatalytic applications; Temperature-Programmed Reduction, Oxidation, and Desorption (TPR, TPO, TPD) for evaluating reducibility, oxygen storage, and adsorption characteristics [49]. These methods often used in combination, providing comprehensive information on the physical, chemical, and structural characteristics necessary to optimize MOF-based catalysts in different applications including BTEX degradation.

3. MOF-based noble metal-supported catalysts

Noble metals such as Pt, Pd, Ag, Au, and Ru supported on conventional supports, such as zeolites, activated carbon and metal oxides like alumina and ceria, have been extensively investigated for BTEX decomposition and details can be found in previous review [50]. Recent research has shifted focus towards utilizing MOFs and MOF-derived materials as supports for noble metal catalysts for BTEX decomposition due to the exceptional properties of MOF-based/derived materials and the catalytic activity of such catalyst matrices [38]. Despite the cost limitation of noble metal-based catalysts, their remarkable low-temperature catalytic efficacy and resilience against deactivation for BTEX oxidation are indisputable [51]. The effectiveness of noble metals-supported catalysts is contingent not solely on the inherent activity of the noble metals but also on the synergy between the supporting materials and noble metal nanoparticles [52]. Hence,

materials exhibiting specific activity can serve as supportive materials in the catalytic process, including but not limited to MnO_x, CeO_x, CoO_x, and others [53]. Inert supports, such as molecular sieves and ceramics, can indirectly enhance catalytic performance by offering a large specific surface area or superior pore structure [54]. Metal oxides obtained from MOFs possess the mentioned advantages and are viewed as promising candidates for support. Furthermore, the steady porous or cage shape of MOFs could serve as a template to control the preparation of nanoparticles, ensuring uniform shape and adjustable size, thereby addressing the nanoparticle aggregation challenge often encountered during annealing process in conventional catalyst synthesis techniques. This is thought to enhance the catalytic efficiency of BTEX oxidation process [55]. This section focuses on the discussion of various noble metal-supported MOF derivatives and metal-based MOFs for BTEX oxidation, especially Ce, Co, and Zr MOF derivative catalysts. Table 1 outlines the preparation techniques and catalytic oxidation capabilities of selected noble metal catalysts supported on MOF or MOF-derived metal oxide, specifically designed for various BTX compounds as no report is available for ethylbenzene degradation over these catalysts.

Noble metals can increase the performance of such kind of catalysts through several ways including electronic effects, synergistic effects, and morphological control. For electronic effects, Noble metals can change the support material's electronic properties, increasing the activation and adsorption of reactants. For instance, Pt can donate electrons to the support, increasing the electron density and thereby improving the degradation of BTEX compounds [56,57]. The catalytic performance of noble metal catalysts supported on MOFs or MOF-derived material can also be enhanced through the synergistic effects between the metal and support. In this case, the combination of noble metals with metal oxides derived from MOFs or MOF itself can create active sites that are more efficient than either component alone. For example, Pd on ZrO_2 derived from MOF can form Pd-ZrO_2 interfaces that facilitate oxygen storage and release, enhancing catalytic performance [58]. Through morphological control, noble metals can control the shape and size of nanoparticles, which are crucial for catalytic efficiency. The porous structure of MOFs can serve as a template for the formation of uniformly shaped nanoparticles, preventing aggregation and maintaining high surface area [59,60].

Despite significant progress, several research gaps remain unsolved. While many studies have demonstrated high catalytic activity in laboratory settings, the long-term stability of these catalysts under industrial conditions remains uncertain. Future research should focus on evaluating the durability and deactivation mechanisms of these catalysts in real-world applications. The preparation of MOF-based/derived noble metal catalysts often involves complex and costly procedures. Developing scalable and cost-effective techniques for the large-scale production of these catalysts is essential [61]. More detailed mechanistic studies are needed to fully understand the role of noble metals and the interaction with MOF supports. Advanced characterization techniques, such as in situ spectroscopy and microscopy, can provide deeper insights into these mechanisms. The environmental impact of using noble metal catalysts, including the potential leaching of metals and the lifecycle analysis of catalyst production and disposal, should be thoroughly investigated.

3.1. Noble metals supported on Ce-MOF and MOF-derived CeO_2 for BTEX oxidation

Cerium (Ce) is a rare earth metal that proves to be highly efficient in catalyzing the removal of BTEX due to the advantageous contribution of the 4 f orbitals in facilitating oxygen vacancy formation [62]. Wang and coworkers [63] explored the impact of different synthesis methods by preparing a range of Ag supported on MOF-derived CeO_2 catalysts, using various approaches. The one-pot synthesis technique involved mixing cerium nitrate and trimesic acid with silver nitrate under solvothermal conditions at 150 °C for 24 h. In post-synthesis, the materials were calcined at 400 °C for 4 h to derive CeO_2 while ensuring the retention of the MOF's structural integrity and enhancing oxygen vacancy generation. The Ag-Ce-BTC-C from one-pot synthesis, demonstrated superior catalytic activity in toluene oxidation, with a T_{90} value of 226 °C. The increased catalytic performance was linked to improved reducibility, increased O_2 vacancies and active O_2 species, an elevated molar ratio of adsorbed and lattice oxygen (O_{ads}/O_{lat}), as well as elevated ratios of Ce^{3+}/Ce^{4+} and Ag^0/Ag^+. The above study offers valuable insights into the development of catalysts derived from MOFs loaded with noble metals.

To gain deeper insight into the impact of MOF structure on the catalytic performance of MOF for BTEX oxidation, three distinct Pt supported on Ce-based MOFs: UiO-66, MOF-BTC, and MOF-808 were prepared using a solvothermal method at 120 °C for 48 h, followed by the impregnation of Pt using a solution-phase reduction technique at 180 °C for 12 h. The Pt/MOF-BTC was calcined at 300 °C for 2 h, leading to its stick-like morphology which significantly influenced its catalytic activity. The ligand utilized in the MOF synthesis process influenced the growth mode of the crystal, leading to diverse coordination of Ce environments and, consequently, distinct catalyst morphologies. Experimental findings revealed that the Pt/MOF-BTC with a stick shape displayed superior catalytic performance compared to the Pt/UiO-66 and Pt/MOF-808 with granular shapes. Moreover, Pt/MOF-BTC showed remarkable resistance to high weight hourly space velocity (WHSV) [64]. The stability of the Pt/MOF-BTC catalytic activity during cycling experiments was attributed to its amorphous structure. However, a more in-depth exploration of the influence of amorphous components on the characteristics of catalysts is needed. The MOF derivative structure is also influenced by the calcination temperature. Thus, adjusting the temperature allows for the effective increase of the specific surface area, providing more sites for precious metals loading [65]. A Mn-Ce oxide composite derived from MOF-supported Pd nanoparticles was prepared by impregnating Mn_3Ce_2 with Pd via an aqueous impregnation technique, followed by calcination at 300°C for 3 h. The impact of a Mn-Ce oxide composite, derived from MOF-supported Pd nanoparticles, was studied for its efficiency in the oxidation of toluene. Through a comparative analysis of experimental outcomes, Pd/Mn_3Ce_2–300 demonstrated remarkable catalytic performance, cyclic performance, stability, and impressive H_2O tolerance (10 wt%). The outstanding performance can be attributed to the substantial presence of Ce^{3+}, Mn^{4+}, O_{ads}, Pd^0, oxygen vacancies, Pd^0, and Pd species abundant on the surface [66].

The formation mechanism of mesoporous CeO_2, synthesized through thermal degradation of Ce-MOF, and its activity for catalytic oxidation of benzene was investigated [65]. Results indicated that Ce-MOF to undergo complete decomposition into pure mesoporous CeO_2 when the degradation temperature exceeds 400°C. At that critical temperature, CeO_2 (400) exhibits the highest specific surface area and largest pore volume. CeO_2 (400) demonstrated exceptional catalytic activity in benzene combustion, achieving complete degradation at 260°C. Furthermore, Pt nanocrystalline catalysts supported on mesoporous CeO_2 (400) were prepared through a high-temperature solution-phase reduction technique and Pt/CeO_2 (400) was capable of entirely degrading benzene at around 200°C, displaying higher durability and water tolerance over a continuous reaction period of 100 h [65].

Based on the existing research, catalysts derived from noble metal-supported Ce-MOF have demonstrated outstanding catalytic efficacy in the oxidation of BTEX compounds at lower temperatures. Nevertheless, limited studies have been conducted, and only two BTEX compounds (toluene and benzene) have been explored. Future investigations could center on studying the oxidation of ethylbenzene and xylenes to broaden the understanding of the catalysts' performance.

3.2. Noble metals supported on Co-MOF and MOF-derived Co_3O_4 for BTEX oxidation

Tricobalt tetraoxide (Co_3O_4) is among the most frequently employed metal oxides for the oxidation of BTEX. The catalytic efficiency of 3D–Co_3O_4 catalysts has been shown as remarkable due to the presence of diffusion-friendly 3D porous channel structures [67]. Hence, multiple approaches have been developed to produce nanostructured Co_3O_4, including the synthesis of nanorods [68], nanotubes [67], and nanoflowers [69]. The catalytic properties of 3D metal oxides produced via the pyrolysis of Co–MOF are notable, and their efficacy can be further improved by incorporating noble metals. Liu et al. [70] fabricated Ru/Co_3O_4-MOF and Co_3O_4-MOF porous materials using MOF-templated approach and evaluated their performance for toluene oxidation. Notably, Ru/Co_3O_4-MOF exhibited superior catalytic activity and CO_2 selectivity compared to Co_3O_4-MOF where toluene complete oxidation was achieved at 240 °C. Li and coworkers [71] reported comparable findings where they synthesized Pd/Co_3O_4 catalysts by incorporating Pd onto a Co_3O_4 porous polyhedron derived from the calcination of ZIF-67. In contrast to Co_3O_4 nanoparticles produced through traditional hydrothermal processes, the resulting catalysts demonstrated a lower T_{90} for benzene (221 °C). The abundant surface-adsorbed oxygen, porous structure, and reducibility were identified as factors contributing to the catalysts' outstanding catalytic activity. The effect of strong electronic interaction between the support and the metal could reorganize internal electrons through the adjustment of chemical bonds and charge transfer within the supported catalyst. This, in turn, leads to alterations in the catalytic performance [56]. To elucidate the electronic metal-support interaction within catalysts derived from Co-MOF, Pt/Co_3O_4 catalysts were prepared for toluene degradation using metal-organic templates. The use of MOFs as templates facilitates electron transfer, resulting in an increased presence of Pt^0 metal species and Co^{3+} species. This robust metal-support electronic interaction enhanced the performance of surface oxygen, the migration capacity of O_{latt}, and the capability to stimulate molecular oxygen, consequently increasing overall catalytic performance [72]. To provide a deeper understanding of these electronic interactions, computational studies like Density Functional Theory (DFT) calculations and spectroscopic methods such as X-ray Photoelectron Spectroscopy (XPS) and Extended X-ray Absorption Fine Structure (EXAFS) can be employed. These techniques can elucidate the charge distribution and electronic states of the noble metal and the support, revealing the nature and extent of electron transfer. The robust interaction of metal and support could be strengthened by incorporating Ce into the Co-MOF template. Simultaneously, the interfacial interaction facilitates the creation of oxygen vacancies, leading to improved Pt dispersion, ultimately enhancing the catalyst's performance [57]. In conclusion, the catalytic efficiency of noble metal supported on MOF-derived Co_3O_4 is interconnected with factors such as the valence state of the precious metal, atomic configuration, support-metal interaction effect, as well as the composition and structure of the support material. The use of computational and spectroscopic studies provides a comprehensive understanding of these interactions, paving the way for the design of more efficient catalysts.

3.3. Noble metals supported on Zr-MOF and MOF-derived zirconia for BTEX oxidation

UiO-66, distinguished by its adaptable pore dimensions and sustained resilience to both thermal and chemical factors, is extensively employed as catalyst support within the diverse array of MOFs [73,74]. Zhang et al. [75] conducted a facile synthesis of silver NPs supported on UiO-66 derivatives for toluene oxidation. Their study involved the preparation of dispersed silver NPs on the UiO-66, and investigating the impact of silver loading on both structure and catalytic activity for the oxidation of toluene oxidation. Interestingly, the structure of 2 wt% Ag/UiO-66 catalyst remained intact, but as the Ag loading increased to 10 wt%, the framework of UiO-66 collapsed, leading to the uniform Ag nanoparticles dispersion on the surface of the support. With a further increase to 14 wt% Ag, larger silver NPs were formed, and silver species migrated to the support's bulk phase, resulting in reduced surface silver content. The 10 wt% silver catalyst exhibited outstanding catalytic activity, which was attributed to its highest surface silver content and lattice oxygen. Additionally, in situ DRIFTS study was employed to investigate toluene-catalyzed intermediates, revealing the conversion of toluene to benzaldehyde and benzoic acid, ultimately forming H_2O and CO_2.

Once again, catalysts comprising single-atom and sub-nanometer clusters of Pd on UiO-66 were synthesized using DMF as a solvent to explore the impact of noble metal atomic scale on the catalytic degradation performance for toluene. The catalysts underwent a preparation process involving calcination in H_2 followed by exposure to an O_2/Ar atmosphere as shown in Fig. 4(a). This continuous pretreatment had the potential to induce linker fracture in UiO-66, leading to the enhancement in specific surface area, thereby favorably influencing catalytic activity.

The cyclic experiment results indicated a substantial improvement in the activity of the catalyst with an elevated number of cycles. The study revealed that benzene ring addition in the reaction gas interacted with nitrogen in the solvent, resulting in Pd single atoms formation in the catalyst, consequently enhancing the catalytic performance. The reconstructed morphology demonstrated stability after three cycles, and the recovered catalyst exhibited high water resistance [76]. The effective design of catalysts with high activity hinges on achieving a significant noble metal nanoparticle dispersion on MOF surfaces [77]. The successful synthesis of Pd NPs supported on UiO-66 with high dispersion was achieved through the ethylene glycol reduction technique (Pd-U-EG) as depicted in Fig. 4(b).

The catalytic activity of these catalysts was assessed through toluene degradation. Notably, even under conditions of higher WHSV, reusability assessments, and stability tests, Pd-U-EG catalytic performance demonstrated no significant changes, affirming its consistent and effective catalytic performance [59]. Developing a universal approach for synthesizing catalysts involving noble metal and MOFs is imperative. In this context, Li et al. introduced a flexible and universal approach for the synthesis of highly dispersed Pd, Pt, and Ru nanoparticles supported on MOFs via the impregnation-reduction technique as shown in Fig. 4 (c).

The developed catalysts were applied for toluene. Metal/MOFs combine MOFs, known for their extensive high porosity and surface area, providing toluene adsorption sites, with highly dispersed metal species that serve as catalytically active sites. Pt/UiO-66 nanoparticles showed excellent CO_2 yield and conversion efficiency of nearly 100 % for the catalytic degradation of toluene at 180 °C. Importantly, there were no noticeable differences in size, morphology, distribution, composition, and crystallinity between used and fresh Pt/UiO-66 nanoparticles, even after a 150-h stability test [60]. These findings offer insights into the development of loaded noble metal catalysts and elucidate the synergistic catalytic mechanism between inert supports and noble metals.

When comparing Zr-MOF catalysts, particularly UiO-66-based systems, to other noble metal-supported MOF catalysts for BTEX degradation, several unique advantages and challenges emerge. Zr-MOF catalysts, especially UiO-66, stand out due to their exceptional thermal and chemical stability, which is crucial for maintaining catalyst integrity during high-temperature oxidation reactions [58,76]. This stability allows for sustained activity even under harsh reaction conditions, a feature not always present in other MOF-based catalysts.

One of the key advantages of Zr-MOF catalysts is their adaptable pore dimensions, which can be tailored to accommodate various BTEX molecules and facilitate their adsorption and subsequent degradation. This flexibility in pore engineering is not as readily achievable with many other MOF systems. Additionally, the strong metal-ligand bonds in Zr-

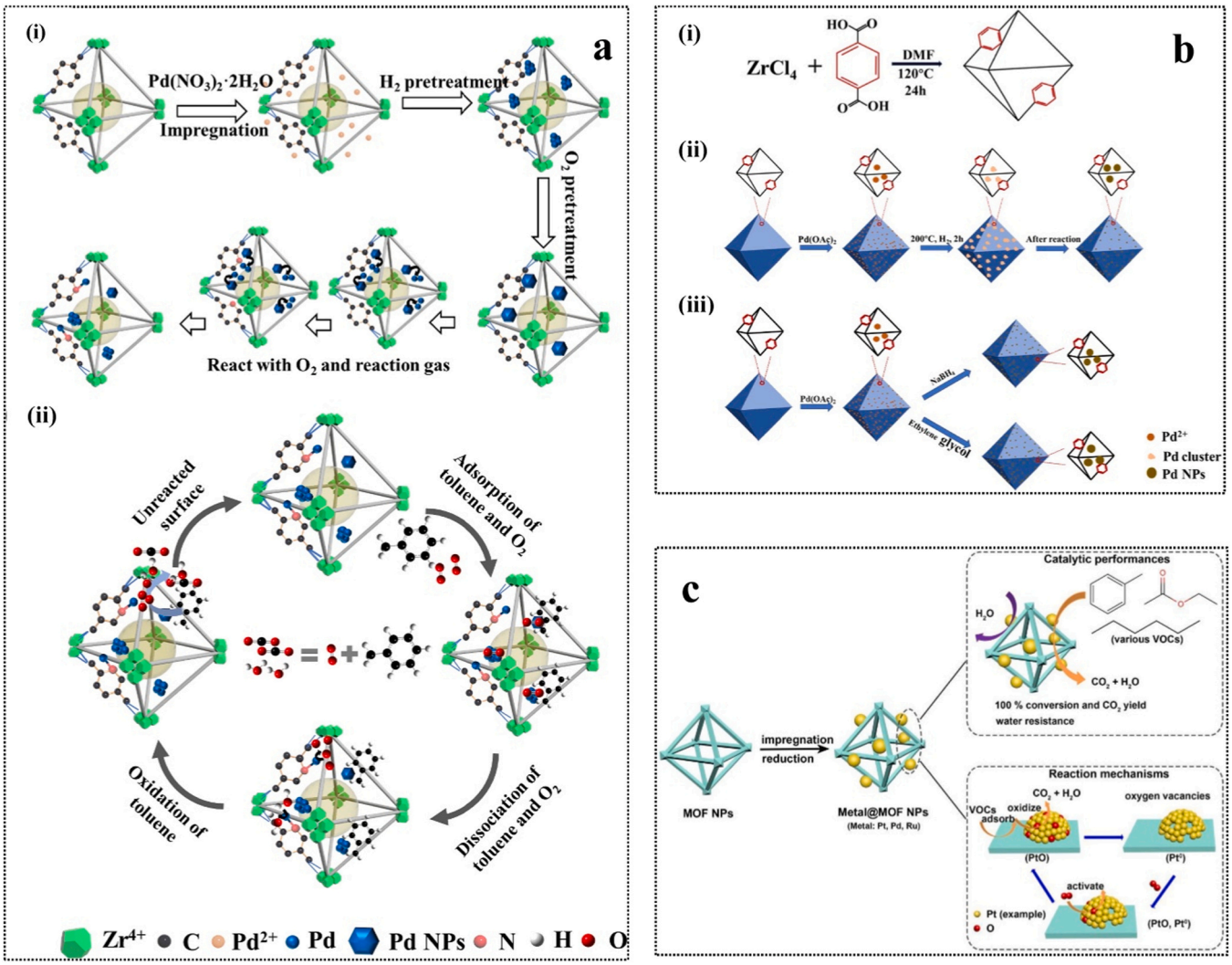

Fig. 4. (a) Scheme of the proposed formation mechanisms for 0.05 Pd–U–H–O–reused (Reproduced with permission from [76]). (b) Schematic of synthesis processes of (i) UiO-66, (ii) Pd-U-H, and (iii) Pd-U-NH and Pd-U-EG. (Reproduced with permission from [59]). (c) Metal/MOFs catalysts exhibited excellent catalytic performance with nearly 100 % conversion efficiency and CO_2 yield as well as good water resistance for the catalytic oxidation of various VOCs including ethyl acetate, n-hexane, and toluene. Besides, VOC molecules were firstly adsorbed on the surface of Pt/UiO-66 NPs as an example and oxidized into CO_2 and H_2O by the lattice oxygen of the PtO. Then, Pt0 with oxygen vacancies was activated by the molecular oxygen and re-oxidized into the PtO to eliminate the oxygen vacancies, forming a Pt^0/PtO redox cycle. (Reproduced with permission from [60]).

MOFs contribute to their robustness, allowing for higher noble metal loadings without framework collapse, as demonstrated in the case of Ag/UiO-66 catalysts [75].

Zr-MOFs also show excellent potential for developing single-atom and sub-nanometer cluster catalysts, as seen with Pd on UiO-66 [76]. This ability to stabilize highly dispersed noble metal species is a significant advantage, potentially leading to enhanced catalytic activity and reduced noble metal usage compared to other MOF-based systems. However, Zr-MOF catalysts face some challenges. The synthesis of highly dispersed noble metal nanoparticles on Zr-MOF surfaces can be more complex compared to other MOF systems, often requiring specialized techniques like the ethylene glycol reduction method. This complexity in synthesis could be a limitation in large-scale applications.

Another challenge is the potential for framework collapse at higher noble metal loadings, as observed with Ag/UiO-66 at loadings above 10 wt% [74]. This limitation might not be as pronounced in some other MOF systems, potentially allowing for higher metal loadings in those cases. When compared to other noble metal-supported MOF catalysts, Zr-MOF systems generally exhibit high water resistance and stability under reaction conditions. This is particularly evident in the case of Pd/UiO-66 catalysts, which maintained high activity even after multiple cycles and showed excellent water resistance [59].

In terms of catalytic activity, Zr-MOF supported noble metal catalysts, such as Pt/UiO-66, have shown exceptional performance for toluene degradation, achieving nearly 100 % conversion at relatively low temperatures (180°C) [78]. This performance is competitive with, and in some cases superior to, other noble metal-MOF systems reported in the literature. Despite these advantages, more research is needed to fully understand and optimize the synergistic effects between Zr-MOFs and noble metals for BTEX oxidation. Future studies should focus on comparative analyses of different MOF supports, including Zr-MOFs, to elucidate structure-activity relationships and further improve catalyst design for BTEX oxidation applications.

In conclusion, the catalytic efficiency of noble metal catalysts supported on MOF or MOF-derived metal oxide, is interconnected with factors such as the valence state of the precious metal, atomic configuration, support-metal interaction effect, as well as the composition and structure of the support material. Furthermore, the production of single-atom catalysts has the potential to minimize the use of noble metals, leading to cost reduction. There is a lack of research specifically

addressing the use of single atom/MOF derivatives in BTEX catalytic degradation. Therefore, exploring this avenue appears to be a promising direction for future studies.

The widespread application of noble metals supported on MOFs/MOF-derived materials has both economic and environmental implications. Although these materials offer promising catalytic properties in applications, challenges emerge owing to their high cost, scarcity, and environmental footprint. Noble metals like Pt, Pd, Rh, and Au are finite resources, and their extraction is often invasive, involving detrimental practices such as open-pit mining. These operations disturb ecosystems, generate large amounts of waste, and need significant energy and water inputs [85]. The energy-intensive nature of mining for noble metals also produces significant greenhouse gas emission, contributing to climate change [86]. Noble metal catalysts often lose their effectiveness over time owing to sintering or poisoning, leading to the production of spent catalysts. If improper disposal occurs, can release toxic metals in the environment. Industrial uses of them also produce waste by-products, some of which are dangerous and pose disposal challenges [87]. Besides, noble metals are costly owing to their scarcity, and large-scale application further strains economic feasibility. Pt and Pd, in particular, have seen significant price variations driven by limited supply and high demand from sectors such as electronics and automotive. Costs related to noble metals enhance production expenses for catalysts, which can be preventive for widespread industrial uses. Again, the availability of noble metals is impacted by geopolitical factors, as they are concentrated in few countries. Supply disturbances can lead to price volatility, affecting industries reliant on these metals for catalytic uses [88,89]. However, various techniques are being explored to decrease reliance on noble metals while maintaining catalytic performance. These strategies includes transition metal based catalysts due to the affordable and availability of transition metals, and exhibit versatile catalytic properties when incorporated in MOFs. These metals can be easily incorporated into MOF frameworks and can be tuned via ligand selection and post-synthetic modifications to optimize performance, potentially offering comparable performance to noble metals [90,91]. Single atom catalysts disperse noble metals at atomic scales on the MOF supports, which significantly decreases the amount of noble metals required while maintaining high catalytic activity. This technique maximizes the use of noble metals by ensuring each atom actively participates in catalytic reactions, improving economic efficiency. Again, combining noble metals with abundant transition metals can reduce the amount of noble metals needed. For instance, Pt-Ni or Pd-Co alloys exhibit synergistic effects, potentially improving stability and performance for specific reactions, while decreasing costs and minimizing resources use [57,81].

To further mitigate the economic and environmental effects of noble metal application, recycling and regeneration techniques for noble metal-based catalysts are critical. Regeneration restores the catalytic performance without the need for complete replacement, converving resources and decreasing waste. Apart from catalyst regeneration, chemical leaching, solvent extraction, thermal and electrochemical recovery, closed -loop recycling systems and use of green solvents for metal recovery are the best strategies for recycling and reusing noble metal based catalysts [86,88].

Although noble metals supported on MOF and MOF derived materials provide significant interests, their environmental and economic cost drive a need for sustainable alternatives and recycling techniques. Single atom catalysts, transition metal based catalysts and biomimetic methods are promising substitutes. For the cases where noble metals remain necessary, recycling, regeneration, and closed-loop processes are critical to minimizing the environmental effects and economic burden. By balancing these techniques, industries can leverage the catalytic advantages of noble metals while promoting sustainability and resources efficiency.

4. Transition metal oxide catalysts derived from MOFs

Transition metal oxides like MnO_x, CoO_x, and CeO_x having abundant active oxygen species, oxygen vacancies, and favorable redox properties, find widespread application in catalyzing the oxidation process of BTEX [92–94]. Furthermore, utilizing MOFs as templates in the synthesizing of these metal oxides provides the added advantage of achieving a higher active centers dispersion [95]. In this regard, metal oxides obtained through the pyrolysis of transition metals-based MOFs exhibit excellent catalytic efficiency in degrading BTEX [96,97]. In this section, we emphasize on examining the impact of catalysts composition on both their physical-chemical characteristics and functionalities. This encompasses a thorough investigation of both monometallic and bimetallic oxides derived from MOF catalysts. Monometallic oxides here are these catalysts derived from MOFs containing a single type of metal ion. They offer simplicity in synthesis and often exhibit high catalytic performance due to the uniform distribution of active sites [90,98]. While bimetallic oxides are those oxides derived from MOFs containing two different metal ions, these catalysts frequently show increased activity through synergistic effects between the two metals [99,100]. Our investigation encompasses a thorough analysis of both categories, exploring how their composition affects their properties and catalytic behavior. Additionally, we have categorized the various methods employed in preparing these catalysts and evaluated their catalytic oxidation capabilities as summarized in Table 2.

4.1. Transition metal oxide catalysts derived from monometallic MOFs

Transition metal oxide catalysts derived from monometallic metal organic frameworks have gained significant concern in recent years due to their potential in variable catalytic applications. Metal-organic frameworks, known for their highest porosity, tunable structures, and well-defined metal sites serves as excellent precursors for transitions metal oxide catalysts. When these metal organic frameworks undergo pyrolysis, the organic linkers are degraded, releasing behind highly dispersed metal oxide nanoparticles within a porous carbon matrix [101]. This process often increases the stability, surface area, and catalytic performance of the resulting transition metal oxides, making them efficient for applications like pollutant degradation, oxidation reactions, and energy storage. With pyrolysis of monometallic MOF, single metal or polymetallic oxides can be produced [102]. The unique properties of MOF-derived transition metal oxides catalysts make the as promising candidates for addressing challenges in sustainable chemical processes and environmental remediation.

4.1.1. Single transition metal oxides derived from monometallic MOFs

Metal oxides derived from a single metal typically lack favorable catalytic properties owing to their physicochemical characteristics. Nevertheless, addressing this limitation to some extent, metal oxides synthesized through MOF pyrolysis offer a solution. The merits of MOF-based catalysts become apparent when their activity is compared with those achieved through alternative methods. Li and coworkers [98] successfully prepared CeO_2 with a MOF structure by pyrolysing Ce-containing UiO-66. In comparison to commercially available CeO_2 and the one prepared through coprecipitation and calcination, MOF-derived CeO_2 exhibits superior activity for catalyzing toluene combustion, achieving a rapid conversion of 100 % within a narrow temperature range. At GHSV of 22500 h^{-1}, the T_{90} values for MOF-derived CeO_2 and conventional CeO_2 were 206 and 322 °C respectively. The outstanding activity of the MOF-derived CeO_2 was owing to its higher concentration of oxygen vacancies, increased surface-active oxygen, enhanced oxidizability, and greater surface acid sites when compared to other CeO_2 forms. X-ray diffraction analysis showed that the MOF-derived CeO_2 maintained the fluorite structure of CeO_2 but with broader peaks, showing smaller crystallite sizes and higher surface area. Transmission electron microscopy (TEM) images

demonstrated that the MOF-derived CeO_2 consisted of nanoparticles with sizes around 5–10 nm, significantly smaller than the conventional CeO_2 particles (>50 nm). This nanostructure, inherited from the MOF precursor, contributes to the increased catalytic performance by providing more accessible active sites. Furthermore, MOF-derived CeO_2 demonstrates better stability and exhibits a comparatively higher level of of water vapor tolerance (5 vol% water). Similar results were found in the work of Chen et al. [90] where CeO_2 was synthesized under atmospheric conditions through the in situ pyrolysis of a Ce-MOF precursor. In comparison to CeO_2 catalysts prepared through precipitation and commercially available ones, catalysts derived from MOFs exhibit outstanding performance in toluene catalytic degradation. Specifically, T_{90} for precipitation-synthesized CeO_2 was 280 °C, whereas the MOF-derived CeO_2 achieved a lower T_{90} of 223 °C. This 57 °C reduction in T_{90} further emphasizes the highest activity of MOF-derived catalysts. The enhanced physicochemical properties contribute to their exceptional catalytic performance and render them highly tolerant to elevated humidity levels (10–20 vol% water).

MOFs represent a class of coordination polymers created through the linkage of metal and organic ligands. Various organic ligands are employed to create distinct structures while maintaining consistent metal connection points. Consequently, the choice of precursors significantly affects the catalytic performance of the resulting catalyst for BTEX oxidation. It is essential to investigate how different ligands influence the structural properties and catalytic performances of MOFs [39]. The synthesis of Mn_3O_4 and Mn_2O_3 catalysts by pyrolyzing two different Mn-based MOF precursors, Mn-BDC and Mn-MOF-74, at various temperatures was reported. The Mn_3O_4 catalyst derived from Mn-MOF-74 calcinated at 300°C showed the best catalytic activity for the oxidation of toluene, achieving T_{90} at 218 °C. XRD patterns revealed that the Mn-MOF-74 derived catalyst maintained a more ordered crystal structure compared to the Mn-BDC derived catalyst, which correlated with its higher catalytic activity. TEM images showed that the Mn-MOF-74 derived catalyst had a more porous structure with smaller particle sizes (20–30 nm) compared to the Mn-BDC derived catalyst (50–70 nm). The hydroxyl groups in Mn-MOFs-74 ligand and optimal pyrolysis temperature played key roles in forming highly active Mn_3O_4 with abundant Mn^{3+}, high O_{ads}/O_{latt} ratio, and good reducibility. It also showed excellent stability and good moisture resistance during a 64-h catalytic test [103]. When compared to conventionally synthesized Mn_3O_4 catalysts, which typically show T_{90} values around 280–300 °C for toluene degradation, the MOF-derived Mn_3O_4 catalyst's activity (T_{90} at 218 °C) represents a significant improvement of 62–82 °C in the T_{90} value. This substantial enhancement in catalytic performance underscores the advantages of using MOF-derived catalysts for BTEX degradation. Similarly, Sun and coworkers investigated how the pyrolysis processes of three different cerium-based MOFs: Ce-MOF-808, Ce-BTC, and Ce-UiO-66 affect the properties and catalytic activity of the resulting cerium oxide catalysts for toluene degradation. It was observed that the destruction of the MOFs during heating to form carbon skeletons that then burn off at higher temperatures significantly impacts the crystallinity, surface area, oxygen storage capacity, reducibility, and number of defects in the final CeO_2 catalysts. XRD analysis showed that CeO_2 derived from Ce-MOF-808 had the broadest peaks, demonstrating the smallest crystallite size among the three catalysts. This was confirmed by TEM images showing Ce-MOF-808 derived CeO_2 had an average particle size of 5–7 nm, compared to 10–12 nm for Ce-BTC and 15–18 nm for Ce-UiO-66 derived catalysts. The smaller particle size correlated with higher catalytic performance. In particular, CeO_2 derived from Ce-MOF-808, which maintained a carbon skeleton over a wider temperature range during pyrolysis, had the smallest particle size, highest surface area, most abundant surface oxygen species, and the greatest number of defects. Consequently, it exhibited excellent catalytic performance for toluene combustion, achieving T_{90} at 205 °C. In comparison, CeO_2 derived from Ce-BTC and Ce-UiO-66 demonstrated T_{90} values of 225 °C and 240 °C, respectively. When benchmarked against conventional CeO_2 catalysts synthesized by precipitation techniques (typical T_{90} around 280–300 °C), the Ce-MOF-808 derived catalyst demonstrated a remarkable improvement of 75–95 °C in T_{90}. This demonstrates the importance of the MOF precursor structure and pyrolysis conditions in designing highly active CeO_2 catalysts [104]. Again, Zhang et al. [105] explored how different MOF precursors and pretreatment methods impact the catalytic activity of resulting manganese oxide catalysts for toluene oxidation. It was found that Mn_2O_3 derived from Mn-MIL-100 and pretreated first in argon and then oxygen (Mn-100-Ar-O) exhibited the highest catalytic performance (T_{100}=270 °C) compared to the one found from Mn-BTC and Mn-MOF-74. XRD patterns demonstrated that the Mn-100-Ar-O catalyst had the most disordered structure, indicating a higher concentration of defects. TEM images revealed that this catalyst had a unique hierarchical porous structure with both meso- and macropores, which was not observed in the other catalysts. This structure provided more accessible active sites and facilitated mass transfer during the catalytic reaction. The highest performance was ascribed to its enhanced low-temperature reducibility, increased surface Mn^{3+}/Mn^{4+} ratio, and higher concentration of surface-adsorbed oxygen species. When compared to conventionally prepared Mn_2O_3 catalysts, which typically achieve T_{100} around 320–350 °C for toluene degradation, the Mn-100-Ar-O catalyst demonstrated a significant improvement of 50–80 °C in T_{100}. Thus, their work demonstrated that the MOF precursor and pretreatment atmosphere significantly affect the catalyst structure and activity.

Current material fabrication methods allow for the preparation of micro-structured materials with controlled shapes, dimensions, and compositions. One area of research is studying how the size of MOF precursors affects the activity of catalysts made by calcining the MOFs. It is also possible to investigate how calcining the same MOF precursor at different temperatures impacts the resulting catalyst's performance [106,107]. Although there have been extensive studies focused on this, the combined effects of using different MOF precursors and calcination temperatures on the catalytic activity have rarely been explored. Additionally, the influence of MOF precursor particle size on the eventual catalyst activity could be examined by pyrolyzing MOF precursors with varied dimensions. While significant research has focused on individual effects, there is an opportunity for new insights by systematically investigating the interconnected impacts of precursor type, calcination temperature, and precursor size on catalytic performance. The synthesis of hollow Co_3O_4 polyhedrons of varying sizes by pyrolyzing MOF precursors was investigated. Co_3O_4 catalysts with different particle sizes were tested for toluene catalytic degradation. It was revealed that the 400 nm Co_3O_4 particles (Co_3O_4-400) demonstrated the highest catalytic performance, with 90 % toluene conversion at 259 °C, compared to 268 °C and 285°C for the 800 nm and 1700 nm particles respectively. XRD analysis demonstrated that all catalysts had the same spinel structure of Co_3O_4, but the Co_3O_4-400 catalyst had slightly broader peaks, showing smaller crystallite sizes. TEM images confirmed the hollow polyhedral structure of the catalysts and revealed that the Co_3O_4-400 catalyst had thinner walls (about 30 nm) compared to the larger particles (50–80 nm wall thickness), providing more accessible active sites. The superior performance of Co_3O_4-400 was ascribed to its high atomic ratio of Co^{3+}/Co^{2+} and more surface-adsorbed oxygen. The Co_3O_4-400 catalyst also showed excellent stability over 30 h of testing [108]. When compared to conventionally synthesized Co_3O_4 catalysts, which typically show T_{90} values around 300–320 °C for toluene degradation, the Co_3O_4-400 catalyst (T_{90} = 259 °C) showed an improvement of 41–61 °C in T_{90}. This demonstrates that controlling the particle size of MOF-derived Co_3O_4 can optimize its catalytic activity for toluene and other BTEX compounds oxidation. Catalysts with abundant oxygen vacancies can adsorb and activate oxygen from the gas phase, enabling the activated oxygen species to partake in catalytic oxidation reactions. As a result, catalysts rich in oxygen vacancies are generally considered more likely to contain reactive oxygen species that can readily facilitate oxidation reactions. It has been demonstrated that appropriate acid

etching can enhance the presence of oxygen vacancies created on the catalyst surface [109]. The addition of tartaric acid during the pyrolysis of Mn-MOF was shown to enhance the development of oxygen vacancies in the resulting MnO_x with rich oxygen vacancies [91]. The catalyst with the optimal ratio of tartaric acid to Mn-MOF (Mn-5TA) showed superior activity compared to MnO_x prepared by traditional methods, with T_{90} of 208 °C for the degradation of toluene. XRD patterns of the Mn-5TA catalyst demonstrated broader and less intense peaks compared to conventionally prepared MnO_x, indicating a more disordered structure with more defects. High-resolution TEM images revealed the presence of numerous edge dislocations and stacking faults in the Mn-5TA catalyst, which were associated with oxygen vacancies. In situ DRIFTS studies demonstrated that oxygen vacancies play a vital role in toluene adsorption and activation during the oxidation process. The Mn-5TA catalyst also had excellent stability for over 30 h. Compared to conventionally prepared MnO_x catalysts, which typically show T_{90} values around 250–270 °C for toluene degradation, the Mn-5TA catalyst (T_{90} = 208 °C) showed a significant improvement of 42–62 °C in T_{90}. Thus, this work provides insights into tuning MOF-derived metal oxides by engineering oxygen vacancies to achieve highly efficient catalytic oxidation of BTEX compounds.

Past investigations have indicated that increasing the redox activity of catalysts can improve their ability to eliminate BTEX compounds. Small amounts of additives like promoters can effectively enhance the redox properties [110,111]. Alkali metals in particular have been reported as good catalyst promoters that can act as electron donors for active site generation. The catalytic activity of alkali metal-doped Mn-MOF for toluene degradation was examined. It was revealed that sodium-doped Mn-MOF derivatives demonstrated excellent catalytic performance due to their large surface area, better oxygen mobility, and lower manganese valence. XRD analysis demonstrated that the sodium doping led to a slight shift in peak positions, showing lattice expansion and the incorporation of Na^+ ions into the MnO_x structure. TEM-EDX mapping confirmed the uniform distribution of Na throughout the catalyst particles. Both adding alkali metals like sodium and introducing H_2O vapor during the reaction promoted the complete toluene mineralization to carbon dioxide and water. The sodium-doped Mn-MOF derivative achieved a T_{90} of 195 °C for toluene degradation, compared to 230 °C for the undoped Mn-MOF derivative. When benchmarked against conventional MnO_x catalysts (typical T_{90} around 250–270 °C), the sodium-doped MOF-derived catalyst showed a remarkable improvement of 55–75 °C in T_{90}. It was concluded that alkali metal doping and water vapor synergistically improve the adsorption and activation of toluene and its intermediates, making these materials promising for BTEX control [112].

4.1.2. Polymetallic oxides derived from monometallic MOFs

Some metal oxides and those obtained from MOFs exhibit insufficient catalytic capabilities for the removal of BTEX. Enhancing these capabilities can be achieved by incorporating guest metals that interact with the MOF's metal sites, thereby improving catalytic performance. Additionally, the method of incorporating these metals plays a crucial role in the catalyst's effectiveness. However, due to the intrinsic characteristics of MOFs, many conventional synthesis techniques are not suitable for creating MOF-derived materials because the MOFs' unique characteristics demand specialized synthesis methods that can precisely control structure, porosity, and other properties while maintaining purity and scalability, which may not be adequately addressed by conventional methods [113]. Impregnation involves submerging a support material with a durable framework into a solution containing secondary metal ions. After a specified duration of interaction, the excess is removed, allowing the active substances to adhere to the support as ions or compounds. This technique is equally applicable to MOFs characterized by their porous architecture [114]. Luo and coworkers synthesized Mn-Co mixed metal oxides derived from MOF precursors for efficient toluene degradation. Catalysts with different Mn/Co molar ratios (1:1, 1:2, and 2:1) were synthesized, and MOF-Mn_1Co_1 (MnCo = 1:1) exhibited the best catalytic performance for total oxidation of toluene. Characterization results revealed that the superior performance of MOF-Mn_1Co_1 was attributed to its uniform nanocubic morphology, higher concentration of surface Mn^{4+} and Co^{3+} species, better low-temperature reducibility, high surface adsorbed oxygen species, and the presence of benzoate route during toluene oxidation [35]. Lei et al. [115] reported the synthesis and characterization of a series of Mn-doped Co_3O_4 catalysts (M-$Co_aMn_bO_x$) derived from Mn-doped Co-MOF (ZSA-1) for toluene catalytic oxidation. The M-$Co_1Mn_1O_x$ catalyst with Co:Mn molar ratio of 1:1 demonstrated superior catalytic performance, achieving 90 % toluene conversion at 227 °C, owing to the increased Co^{3+} formation, surface adsorbed oxygen species (O_{ads}), and the synergistic impact between Mn and Co. Characterization techniques revealed that M-$Co_1Mn_1O_x$ possessed small particle size, high specific surface area, more lattice defects, and higher reducibility compared to undoped Co_3O_4. This demonstrates that Mn doping of Co-MOF is an effective technique to increase the catalytic performance of Co_3O_4 for toluene oxidation. Similarly, Han and coworkers also showed that introducing Mn effectively restricts the development of Co_3O_4 nanoparticles and disrupts the catalyst's structure which led to defects creation in the structure. The catalysts were developed by depositing Mn onto the surface of the Co_3O_4 spinel structure, with the incorporation of Mn causing lattice distortions. This process leads to the formation and exposure of active sites that enhance catalytic performance [116]. Encasing metal atoms within the cavities of a stable MOF host can successfully prevent the clustering of active metals that typically occur during the pyrolysis process [115]. For instance, Chen and coworkers reported the fabrication of MnO_x/Cr_2O_3 composites through a series of techniques involving impregnation, in situ redox precipitation, and subsequent pyrolysis. The incorporation of an additional metal improves the catalyst's oxygen storage capability, oxygen mobility, and reducibility, thereby benefiting its catalytic performance. The prepared catalysts exhibited T_{90} at approximately 268 °C at 20,000 h^{-1} space velocity (SV) and a concentration of 1000 ppm toluene [100]. Similarly, Li et al. [117] reported a dual confinement technique based on MOFs to prepare MnO_x@ZrO_2 catalysts for catalytic degradation of toluene. The MnO_x nanoparticles were well-dispersed on the c-ZrO_2 support through spatial confinement in MOF-808 cavities and carbon confinement from pyrolysis. The MnO_x@ZrO_2-NA catalyst exhibits excellent toluene oxidation performance with T_{50} of 248 °C and T_{90} of 288 °C, outperforming the conventionally prepared catalysts. High activity was attributed to the reduced aggregation of MnO_x, enhanced Mn (III/total) ratio, adequate O_{ads} species, and better oxygen mobility from the support (c-ZrO_2). The dual confinement strategy is demonstrated to be effective and versatile for preparing highly dispersed metal oxide catalysts for BTEX removal. Utilizing $KMnO_4$ in the impregnation method proves beneficial as it facilitates the etching and oxidation of MOFs during the process of assembly. Specifically, $CoMn_6$ catalysts were examined, showcasing enough mesoporous structure and even distribution of cobalt atoms formed through oxidation–etching. The robust interaction between the two components in the preparation phase generates numerous oxygen vacancies and defects, contributing significantly to the catalyst's superior activity for toluene oxidation [118].

The inherent structure of the parent MOF significantly influences the characteristics of its resulting metal oxides. Catalysts with distinct dimensional structures exhibit varied activities towards BTEX compounds, prompting extensive research on the structure-activity relationship [119,120]. In one study, Han et al. examined three catalyst morphologies produced through electron spinning and CoMn-MOF pyrolysis. 1D In–$CoMnO_x/MnO_y$ bead chain-like, grown on Polyacrylonitrile (PAN) from the precursor of CoMn, displayed optimal catalytic activity (T_{90} = 200 °C) compared to 2D and 3D structured materials. Characterization by XRD and TEM revealed the bead chain-like structure had a robust bimetal synergy impact, increased oxygen vacancies, and a higher concentration of weak acid sites, which

contributed to its highest performance [121]. Similarly, Han et al. synthesized $CeCoO_x$ catalysts with one-dimensional NPs, two-dimensional hexagonal nanosheets, and three-dimensional rosette-like structures via one-step hydrothermal technique. The three-dimensional mesoporous rosettes-like catalysts demonstrated the highest toluene catalytic performance ($T_{90} = 168\ ^\circ C$) owing to its larger pore size, more oxygen vacancies, and increased O_{ads} on the surface as confirmed by N_2 adsorption-desorption, XPS, and O_2-TPD analyses [122].

Hydrothermal technique is frequently employed for MOF synthesis due to its capability to regulate crystallinity and particle size [123]. However, it requires high temperatures and extended reaction times can result in energy waste and inconvenience. The mechanical grinding method circumvents these drawbacks, allowing large-scale production [99]. Additionally, using EDTA as a grafting ligand instead of formic acid in the synthesis of MOF-808 facilitates the production process. Sun et al. demonstrated that mixing and homogenous grinding of $CuAc_2$, EDTA, and Ce–MOF–800 led to the formation of atomically dispersed copper atoms on Ce–MOF–808, which promotes the catalytic elimination of toluene [124]. Overall, both monometallic and polymetallic catalysts derived from monometallic MOFs exhibit excellent oxidation performance towards BTEX compared to those synthesized through traditional techniques. The significant specific surface area and unique morphologies of MOF derivatives, provides numerous active sites which benefits the active metals dispersion of active metals and tailored mass transport properties, leading to superior catalytic performance compared to traditional catalysts for BTEX removal. Moreover, the choice of organic ligands influences the product's morphology and, consequently, pollutant diffusion, impacting the overall catalytic activity.

4.2. Transition metal oxide catalysts derived from bimetallic MOFs

These types of catalysts represent an advanced class of materials with improved catalytic properties and structural stability. Bimetallic metal-organic frameworks, which incorporate two different metal ions within a single framework, provide unique synergies between metals that can optimize catalytic activity [35]. Through pyrolysis, these metal organic frameworks transform into bimetallic oxide catalysts, often featuring a homogenous distribution of metal oxides or mixed-metal oxides embedded in a porous carbon matrix. This dual-metal system offers enhanced redox properties, high active site diversity, and improved resistance to sintering compared to their monometallic counterparts [125]. These attributes make bimetallic MOF-derived transition metal oxides particularly effective in challenging applications like selective catalytic reduction and different environmental remediation processes. As a result, these catalysts exhibit great promise in developing sustainable catalytic technologies.

4.2.1. Core-shell structured catalysts

Catalysts with core-shell structures have emerged as a promising method to enhance catalyst activity and reduce costs. Specifically, core-shell structured catalysts utilizing two metals offer a means to optimize the utilization of one metal in the shell. Additionally, this approach aids in improving catalytic activity by inducing electronic alterations and minimizing metal segregation within bimetallic structures [26,126,127]. The extensive functional range of pristine MOFs can be broadened by incorporating a framework guest into the second framework, allowing for the modification of electronic structure and activation properties through core-shell interactions [128]. Various metal oxides exhibit varying tolerance and selective catalytic properties towards BTEX compounds. Consequently, a more resistant metal may serve as a shell, while a more reactive metal may function as a core for creating bimetallic MOFs. Core-shell material based on two metals not only retains the advantages of each metal but also generates synergistic impacts [129]. In this approach, a MOF core is typically prepared first, followed by the formation of a shell MOF around it, akin to "encasing a ship in a bottle" [130]. The resulting three-dimensional core-shell structure offers a high surface area. For instance, Gu and coworkers produced novel Co-MOF–74@Mn–MOF-74 core-shell samples with varying thicknesses of the shell by controlling precursor mass ratios. The core-shell structure of the catalysts was confirmed through extensive characterization. Scanning electron microscopy (SEM) and transmission electron microscopy (TEM) analysis revealed the presence of a distinct core-shell morphology, with the shell material uniformly coating the core. Elemental mapping using energy-dispersive X-ray (EDX) spectroscopy further confirmed the spatial distribution of the two metal components, showing the core-shell architecture. The core-shell structured catalysts exhibited higher catalytic activity compared to their single-component counterparts. For toluene oxidation, the Co-MOF-74@Mn-MOF-74 core-shell catalyst demonstrated significantly higher toluene conversion rates, reaching over 90 % at temperatures below 300°C. This enhancement was attributed to the synergistic effects between the core and shell materials, which facilitated improved oxygen activation and adsorption of the reactants. The catalysts also showed excellent selectivity, with benzaldehyde being the primary oxidation product. Moreover, the core-shell structure provided improved stability, with the catalyst maintaining its activity over extended periods of operation [131]. At lower temperature, oxygen activation rate on Co_3O_4 may be insufficient, leading to the intermediates deposition on the active sites and deactivation of the catalyst. The addition of Mn effectively promotes the oxygen activation ability of Co_3O_4. Additionally, the inherent characteristics of Co_3O_4 spinel oxides can be enhanced by replacing the non-active Co^{2+} ions with other active transition metal cations. The Co_3O_4@$CoMn_2O_4$ hierarchical hollow structured catalyst was reported. It was found to exhibit an excellent toluene oxidation performance attributed to its higher specific surface area and improved diffusion and adsorption of pollutants with the hierarchical hollow structure [132].

The synergistic effects between poly-metals in core-shell structures effectively suppress the formation of by-products and catalyst poisoning. For example, three catalysts with core-shells were prepared. $CoCuO_x$ dodecahedron acted as the core and CeO_2, TiO_2 and Nb_2O_5 functioned as shells, enriching surface lattice oxygen and acidic sites, conducive to catalytic degradation for benzene. The shell protects the core from active site poisoning, facilitating the conversion of benzene to the end product. Furthermore, investigations have demonstrated that the core-shell structure enhances toluene oxidation by adjusting oxygen activation and adsorption strength [133]. This insight provides a way for understanding the relationship between various metals and the catalytic combustion of typical BTEX through various metal structures, offering an effective approach for designing catalysts with superior oxidative activity against target pollutants. Nevertheless, limited studies have been conducted, and only some types of BTEX compounds (toluene and benzene) has been explored. Future investigations could center on studying the oxidation of other BTEX compounds over bimetallic core-shell structured catalysts.

4.2.2. Aliovalent substitution

Aliovalent substitution, commonly known as heterovalent substitution, refers to the process wherein ions of one element within a crystal lattice are replaced by ions of another element with a different valence or oxidation state. The essence of aliovalent substitution lies in the exchange of ions with disparate charges, inducing alterations in the crystal structure and impacting the material's electrical and structural attributes [134]. Aliovalent substitution becomes feasible by introducing a metal with a dissimilar valence during the fabrication of a specific MOF because various metals can react with identical organic linkers. In the MOF formation process, the addition of the desired second metal facilitates molecular-level mixing of MOF precursors, enhancing the material's oxygen storage capacity and redox activity without inducing phase separation in the resulting metal oxides [135]. Bimetallic oxides, produced through aliovalent substitution, typically exhibit superior catalytic activity compared to their monometallic MOF counterparts. The

substitution of metal ions in the lattice creates structural defects, such as oxygen vacancies, which are critical for catalytic performance. For instance, cerium oxide, considered a promising heterogeneous catalyst, is chosen for its high redox capacity, widespread availability, and non-toxicity. Introducing Ce into Co-based catalysts, through aliovalent-substitution of Co into the CeO_2 lattice, results in the formation of a stable half-filled orbital leading to an increased number of oxygen vacancies. These vacancies act as active sites for the adsorption and activation of reactant molecules, significantly enhancing catalytic activity [136]. Spectroscopic analysis, such as X-ray photoelectron spectroscopy (XPS) and in-situ Fourier transform infrared (FTIR) spectroscopy, reveals that aliovalent substitution induces shifts in the valence states of the metal ions, facilitating electron transfer processes that are crucial for redox reactions. Additionally, computational studies, including density functional theory (DFT) calculations, can predict the energy barriers for these reactions, providing insights into how aliovalent substitution decreases activation energies and increases reaction kinetics. Achieving stable CoCe-MOF crystals involves mixing Co and Ce atoms at the atomic level during the preparation process. For instance, the development of a $CoCeO_x$ catalyst derived from a bimetallic CoCeBDC (benzenedicarboxylic acid) MOF precursor was reported. The spectroscopic analysis confirmed the successful aliovalent substitution of Co into the ceria lattice, creating defects and oxygen vacancies. For toluene oxidation, the $CoCeO_x$ catalyst achieved 50 % conversion at 212°C and 90 % conversion at 227°C, outperforming a reference Co_3O_4/CeO_2 nanocube catalyst (T_{50} = 261 °C, T_{90} = 308 °C). The $CoCeO_x$ catalyst also showed high activity for the oxidation of other BTEX like o-xylene. The enhanced catalytic performance was ascribed to the uniform incorporation of Co into the ceria lattice enabled by the MOF synthesis approach [134].

The pyrolysis-derived metal oxides from bimetallic MOFs offer distinct benefits compared to traditional preparation approaches. CeMn bimetallic oxides, resulting from this process, exhibit outstanding catalytic activity towards BTEX compounds owing to their elevated oxygen storage capacity and enhanced dispersion of transition metal oxides [137]. The fabrication of MnO_x and MnO_x-CeO_2 catalysts derived from MOF precursors for catalytic toluene degradation was reported. The MnO_x-CeO_2-MOF catalyst synthesized by pyrolyzing a Ce/Mn-MOF-74 precursor showed higher catalytic activity compared to MnO_x-MOF, MnO_x-CeO_2-CP (co-precipitation method) and MnO_x-D (from MnOOH) catalysts. The MnO_x-CeO_2-MOF catalyst had higher surface area, abundant oxygen vacancies, highest oxygen mobility, and excellent surface Mn^{4+} content which contributed to its superior performance [138]. The MOF-derived catalysts outperformed those from conventional preparation methods, demonstrating the advantage of using MOF as precursors. Chen et al. [139] developed MOF-derived MnCeOx catalysts for low-temperature catalytic degradation of benzene. The Mn_1Ce_1-MOF catalyst synthesized by a solvothermal approach showed the best performance, achieving 90 % conversion at 242 °C due to its microporous structure, high lattice oxygen content, and good reducibility.

Studies have indicated that diverse metal substitutions during MOF synthesis can demonstrate varying catalytic activities against BTEX pollutants, surpassing those observed in mixed metal oxides produced through traditional co-precipitation techniques [140]. The substantial catalytic effectiveness can be linked to alterations in the valence state of the species induced by electron transfer. During the catalytic conversion of BTEX, acidic sites demonstrate a robust capacity to activate C–H bonds. Lewis acids are more preferred as they are able to accept electron pairs due to the presence of vacant orbitals. When a Lewis acidic site interacts with a C-H bond, it typically involves coordination of the Lewis acid with the C-H bond, leading to polarization of the C-H bond. This polarization makes the hydrogen atom more electrophilic, making it more susceptible to nucleophilic attack or other reactions. Therefore, incorporating a specific quantity of acidic sites into the catalyst proves advantageous for promoting the catalytic reaction. Among various preparation approaches, metal ion doping emerges as an efficient method for introducing acidic sites. Guo et al. [141] reported the catalytic degradation of BTEX compounds including toluene and benzene using metal oxide catalysts derived from bimetallic zeolitic imidazolate frameworks (ZIFs). In their work, ZnCo-ZIFs with different Zn/Co ratios were synthesized and then pyrolyzed at 350°C to obtain $ZnCoO_x$ catalysts. Among them, $Zn_{0.05}CoO_x$ with 5 % Zn doping exhibited the best performance for eliminating the two BTEX compounds under simulated exhaust conditions containing 5 % water vapor. This was attributed to its high concentration of acid sites, good reducibility, and strong Co-Zn interaction. The $Zn_{0.05}CoO_x$ catalyst also showed excellent stability over 30 h. Those results provide new insights into designing highly efficient catalysts from MOFs and understanding the impact of BTEX chemical structures on catalytic oxidation processes. Similarly, Wang et al. [142] reported the synthesis of Sm-doped CeO_2 catalysts by pyrolyzing MOF precursors containing Sm and Ce. It was found that doping small amounts of Sm into CeO_2 led to more oxygen vacancies and improved reducibility compared to undoped CeO_2. Among the Sm-doped CeO_2 catalysts, 1 % Sm/CeO_2 showed the highest catalytic activity for toluene degradation, with T_{50} = 194°C and complete conversion at 222 °C under certain conditions. The excellent catalytic performance was attributed to a higher concentration of defects, oxygen vacancies, and Ce^{3+} species caused by optimal Sm doping, which enhanced the redox properties and oxygen mobility. The 1 % Sm/CeO_2 catalyst also showed good long-term stability and moisture tolerance.

The thermal fragility of organic linkers often leads to the structural breakdown of MOF-based catalysts under high-temperature conditions. Conversely, UiO-66 exhibits notable hydrothermal and chemical robustness at elevated temperatures, attributed to its high coordination number and unique pore configuration [143]. Past research has rarely explored how varying metal dopants influence the efficacy of Ce-MOF-based catalysts that have been synthesized. Currently, UiO-66-Ce has been altered with the addition of Cu, Co, Mn, Fe, and Zr using a single-step synthesis technique. In this process, Cu substitutes Ce in its octahedral arrangement, facilitating an electron transfer reaction. As a result, the CeCu-MOF exhibits enhanced redox capabilities. Moreover, the synergy between Ce and Cu significantly increases oxygen vacancies, improving both the activity and selectivity of the products [144]. Additionally, the physicochemical characteristics of these MOF derivatives can be tailored by varying the synthesis conditions. By manipulating the alteration temperature, it's possible to regulate the size and volume of the internal voids, which in turn allows for the control of particle size and surface area [145]. Zhang and coworkers investigated the impact of varying calcination temperatures on the catalytic efficiency of $MnCeO_x$ catalysts for the degradation of toluene. They found a performance sequence with 1Mn1Ce–300 (T_{90}, 244 °C) being more effective than 1Mn1Ce–400 (T_{90}, 264 °C) and 1Mn1Ce–200 (T_{90}, 283 °C), and the lowest efficiency was observed with 1Mn1Ce–500 (T_{90}, 298 °C). The study revealed that the calcination temperature significantly influences the catalysts' specific surface area, pore volume, and particle size. These physical changes subsequently affect the catalysts' metal valence states, the concentration of oxygen vacancies, and their capacity for reduction. Specifically, the 1Mn1Ce–300 variant showed an enhanced ability to facilitate toluene oxidation by effectively utilizing lattice oxygen in conjunction with gaseous oxygen [146]. 2D materials are distinguished by their exceptional anisotropic and electronic characteristics, making them highly suitable for catalytic applications. These materials can be engineered through in situ topological methods or by utilizing layered hydroxides as starting materials [147, 148]. Wang and coworkers [149] developed 2D structured MOFs through a solvothermal approach, leading to the synthesis of bimetallic oxides $CeCuO_x$ upon calcination. The strategic insertion of copper into the ceria framework introduces a higher density of oxygen vacancies, facilitating the efficient conversion of toluene to CO_2. This transformation is believed to be driven by the dynamic exchange among Cu^+, O_v, and Ce^{3+}, attributing to the material's pronounced catalytic performance, especially in processing BTEX compounds. The exposure of

the (100) crystal planes further enhances the material's stability and resistance to water by minimizing surface reactivity, providing a more inert surface, and potentially imparting hydrophobic characteristics. Ultimately, molecular-level integration during synthesis fosters the creation of catalysts characterized by structural defects and robust redox capabilities, significantly enhancing their catalytic efficiency.

Optimizing these catalysts involves carefully balancing the metal ratios and processing conditions to maximize the number of active sites while maintaining structural stability. One of the primary challenges is controlling the distribution of aliovalent metal ions within the lattice to avoid agglomeration, which can lead to reduced catalytic efficiency. This challenge is compounded by the fact that various metals have varying affinities for the MOF precursors, leading to inhomogeneous distributions. Potential solutions include the utilization of advanced synthesis methods such as atomic layer deposition (ALD) or template-assisted methods that can provide better control over metal distribution at the atomic level. Furthermore, maintaining the stability of the catalysts under reaction conditions, especially at high temperatures, is another significant challenge. The thermal fragility of organic linkers in metal-organic frameworks can lead to structural breakdown, reducing catalyst activity over time. Strategies to increase stability include the development of more robust MOF structures with higher coordination numbers or the incorporation of stabilizing agents that can preserve the framework integrity under harsh conditions.

For instance, the development of $CoCeO_x$ catalysts derived from a bimetallic CoCeBDC (benzenedicarboxylic acid) MOF precursor demonstrated increased catalytic activity for toluene degradation. The spectroscopic analysis confirmed successful aliovalent substitution, with the Co incorporated uniformly into the ceria lattice, creating defects and oxygen vacancies that contribute to higher catalytic performance. The $CoCeO_x$ catalyst achieved 50 % conversion at 212 °C and 90 % conversion at 227 °C, outperforming a reference Co_3O_4/CeO_2 nanocube catalyst. The enhanced activity is attributed to the MOF preparation approach, which ensures uniform metal distribution and maximizes the number of active sites [134].

Additionally, MnO_x-CeO_2 catalysts derived from MOF precursors exhibited higher catalytic activity due to their large surface area, abundant oxygen vacancies, and high oxygen mobility. The Mn1Ce1-MOF catalyst, for example, demonstrated the best activity with 90 % benzene conversion at 242 °C. The high lattice oxygen content and good reducibility of these MOF-derived catalysts highlight the role of optimizing preparation conditions, such as calcination temperature, to tailor the physicochemical properties of the catalyst for enhanced activity [138].

In conclusion, while aliovalent substitution offers significant potential for enhancing catalytic activity, optimizing these materials requires a comprehensive understanding of the underlying mechanisms and addressing challenges related to metal distribution, structural stability, and process scalability.

Weight hourly space velocity (WHSV), defined as the volumetric flow rate of reactants per unit weight of catalyst (mL/(g·h)), is an important factor influencing the efficiency of MOF-based and derived catalysts for BTEX oxidation [26]. WHSV directly affects the contact time between reactants and catalysts, thereby impacting conversion efficiency, selectivity, and reaction kinetics. Lower WHSV means longer contact time. A lower WHSV provides a longer residence time for BTEX molecules on the surface of the catalyst, allowing more effective adsorption and oxidation. A lower WHSV increases intermediate oxidation processes, leading to higher CO_2 selectivity and fewer by-products. Higher WHSV means shorter contact time. At higher WHSV, the reduced contact time results in lower oxidation efficiency, as reactants may not fully interact with active catalytic sites. For instance, when WHSV increased from 30,000 to 60,000 mL/(g.h), the T_{90} of $Pd@ZrO_2$ catalysts shifted up to 50 °C higher [58]. In some cases, catalysts with hierarchical or mesoporous structures such as $CoMnO_x$ compensated for the reduced residence time by increasing reactant diffusion and oxygen mobility [118].

Apart from WHSV, the amount of catalyst used plays a crucial role in determining its efficiency in BTEX oxidation. This is particularly relevant for MOF-derived catalysts, where the dispersion of active sites and accessibility to reactants depend on catalyst morphology and loading. A sufficient catalyst amount ensures adequate surface-active sites for the adsorption and oxidation of BTEX [169]. Increasing the catalyst loading beyond the optimal amount does not necessarily enhance the performance owing to mass transfer limitations and reactant diffusion constraints. High catalyst loading could lead to the blockage of pores, reducing the effective surface area and catalyst utilization. Excess catalyst amounts may result in the accumulation of heat, promoting undesirable side reactions or structural degradation. For instance, Pt/MOF-800 showed that exceeding 0.2 g catalyst loading did not yield significant enhancements in BTEX oxidation efficiency [64]. At insufficient catalyst loading, active sites may be saturated with reactants, leading to incomplete oxidation. This effect is more pronounced at high WHSV, where rapid reactant flow overwhelms the limited catalytic surface. For instance, $Pd@Co_3O_4$ exhibited 20–30 % lower BTEX conversion when the catalyst loading was reduced from 0.1 to 0.05 g [71].

The interplay between WHSV and catalyst loading determines the optimal operating window for MOF-based and derived catalysts. Lower WHSV with higher catalyst loading facilitates maximum conversion but may cause mass transfer limitations. Higher WHSV with lower catalyst loading facilitates reduced efficiency owing to insufficient residence time and active site saturation. However, moderate WHSV and optimized catalyst loading lead to the best balance between reactant flow and catalyst utilization.

Optimizing WHSV and catalyst loading is crucial for enhancing the oxidation of BTEX over MOF-based catalysts. For practical applications, catalysts should be evaluated under a range of WHSV conditions to ensure robust performance under real-world operational constraints. Future research should explore hierarchical MOF structures and single-atom catalysts, which can maintain high activity even under high WHSV conditions.

5. Impact of H_2O and SO_2 on the performance of catalysts derived from MOFs

The presence of water and SO_2 in industrial emissions is a critical concern because these compounds can lead to catalyst deactivation, reducing the efficiency of BTEX degradation. They are prevalent constituents found in industrial gas emissions, and are unavoidable in practical exhaust gases. These substances influence the catalytic efficacy of catalysts derived from MOFs [39,83]. A thorough comprehension of the impacts of H_2O and SO_2 function on the oxidation process will facilitate the design of more poisoning-resistant catalysts for practical abatement of BTEX. In general, the impact of a low water vapor content (less than 3 vol%) on the catalytic activity is typically insignificant and may even lead to performance enhancement [59,60]. The introduction of water can effectively remove intermediates adsorbed on the surface of the catalyst, exposing previously enveloped active sites [178]. Water vapor can also generate OH^- groups, serving as surface O_{ads} species believed to promote the oxidation of BTEX compounds [112]. Toluene degradation was investigated under wet conditions through an in situ DRIFTS examination. The presence of water increased the peak of maleate species, demonstrating that wet conditions facilitated the opening of the ring of toluene [179]. Previous research showed that catalysts with sufficient oxygen vacancies facilitate the conversion of adsorbed oxygen to lattice oxygen, a key reactive species promoting ring-opening [180,181]. The introduction of water vapor was found to accelerate oxygen species conversion, thereby increasing the catalytic performance by promoting the opening of the ring. Additionally, H_2O vapor influences CO_2 selectivity. Some studies revealed that H_2O vapor introduction led to contaminants mineralization, resulting in higher CO_2 production compared to dry air conditions. In this case, the introduction

of H_2O vapor promotes the mineralization of organic contaminants into CO_2 through oxidation reactions facilitated by the presence of reactive oxygen species and hydrolysis processes. This can result in higher CO_2 production compared to dry air conditions, where the oxidation of contaminants may proceed at a slower rate or through different pathways. That is why H_2O vapor reduced by-product formation and enhanced CO_2 selectivity [109,112]. The intermediates reduction and the increment in surface OH^- groups promoted the process of mineralization, this could be attributed to the creation of particular sites for water adsorption, leading to a reduction in the effectiveness of water adsorption without dissociation. Water molecules act as active sites for HOH on vacancies in oxygen, transforming adsorbed oxygen into a lattice. The CO_2 yield is reversible after removing water vapor, indicating the reversibility of its influence [112]. However, as the water content further elevated (typically > 5 % vol), catalytic activity might decline. This decline was attributed to the competitive water adsorption, occupying oxygen vacancies and reducing reactive O species. The intermediate product accumulation hindered additional deep contaminants oxidation [152]. Nevertheless, that deactivation proved reversible upon cessation of H_2O vapors introduction, highlighting the potential for recovery [96]. It's worth noting that both moisture content and operating temperature play a role in benzene catalytic activity. Stability tests at 140°C demonstrated that the catalytic performance was less negatively affected at elevated temperatures as shown in Fig. 5. The catalyst's ability to adsorb much benzene with oxygen species in wet conditions at elevated temperatures contributed to this observation [182].

Bi and coworkers [83] investigated how H_2O and SO_2 affect the performance of ultra-low palladium catalysts supported on UiO-66 and related materials for toluene oxidation. The presence of H_2O impeded the breakdown of toluene and the production of CO_2 over the supported Pd catalysts. When examining the time-dependent conversion of toluene and CO_2 yield during toluene oxidation over different catalysts such as Pd-U, Pd-U-NH_2, Pd-U-NO_2 (Fig. 6), the addition of 5 % vol H_2O significantly decreased the catalytic activity of the Pd-supported catalysts, highlighting the substantial impact of water vapor. However, after discontinuing the H_2O vapor, toluene conversion and CO_2 yield gradually recovered, indicating the reversible nature of its adverse effects. Increasing the H_2O vapor to 10 % volume did not exacerbate its negative impact, likely due to the lower and unstable catalytic activity of the catalysts initially. The rapid restoration of catalytic performance after ceasing water vapor confirmed that the competition for adsorption between H_2O vapor and toluene on the catalyst was the main factor causing the decline in catalytic performance.

The impact of SO_2 on the same catalysts was also examined. Increasing concentrations of SO_2 led to a gradual decline in toluene conversion and CO_2 yield over Pd-supported catalysts, particularly notable at lower temperatures. This adverse effect was consistent across varying SO_2 concentrations (Fig. 7). Notably, differences were observed among the three Pd-supported catalysts, with Pd-U-NO_2 showing distinct behavior. While Pd-U and Pd-U-NH_2 exhibited recoverable catalytic activity after SO_2 exposure, Pd-U-NO_2 experienced irreversible deactivation, suggesting SO_2 poisoning as the primary cause. Adsorption of SO_2 on the catalyst surface was speculated to be the main contributing factor to this deactivation.

Brandt and coworkers [183] observed that incorporating the NH_2 group linker in comparison to MIL-53(Al) and MIL-101(Al) enhanced the affinity of the material for SO_2. Li et al. [184] conducted a simulation study to calculate the adsorption isosteric heat of UiO-66, UiO-66–NH_2, and UiO-66–NO_2 for sulfur dioxide. The high adsorption isosteric heat value shows higher interactions between absorbed gas and materials. The isosteric heat of the adsorption sequence for SO_2 on three catalytic materials is UiO-66–NO_2 > UiO-66–NH_2 > UiO-66, indicating the highest interaction between SO_2 and –NO_2. Furthermore, Zhang and coworkers [185] employed molecular simulations to calculate the SO_2 adsorption for functional aromatic frameworks and revealed that the group of NO_2 exhibited superior uptake of SO_2 gas compared to the group of NH_2. Therefore, designing a MOF-derived catalyst with fewer or no NO_2 groups could be advantageous in preventing catalytic deactivation induced by SO_2.

These reports present innovative approaches to develop water and SO_2-resistant catalysts derived from MOFs, with the goal of developing stable catalysts for BTEX oxidation. However, there is limited research on how H_2O and SO_2 impact the catalytic efficiency of MOF-derived catalysts. Further studies are necessary, particularly regarding the SO_2 influence on the catalytic activity of MOFs-based and derived catalysts for BTEX oxidation. Existing research primarily emphasizes the effects of water, and additional investigations are warranted to address the scarcity of information on SO_2 effects.

To mitigate the negative effects of water and SO_2 on catalyst activity, various strategies can be considered including surface modification, hydrophobic coatings, dual functional catalysts, and operational adjustment. Modifying the surface of MOF-derived catalysts to reduce the affinity for SO_2 adsorption can help minimize deactivation. For example, designing catalysts with fewer or no NO_2 groups could prevent SO_2-induced poisoning, as these groups have shown higher interaction with SO_2. Applying hydrophobic coatings to the catalyst surface could limit water adsorption, reducing competitive adsorption at high concentrations of water. This approach would maintain active oxygen sites available for BTEX degradation, thereby sustaining catalytic performance even in humid conditions. Developing catalysts with dual functionality, where specific sites are tailored for SO_2 and water resistance, can enhance overall performance. For instance, incorporating both hydrophobic and SO_2-tolerant components in the catalyst design could ensure better resistance to these pollutants while maintaining high catalytic efficiency. Adjusting operational conditions, such as increasing the operating temperature, can also mitigate the adverse impacts of water and SO_2. Higher temperatures may enhance the SO_2 desorption and reduce the negative effects of water by maintaining the catalyst's performance through improved oxygen vacancy availability.

Future research should focus on these mitigation strategies,

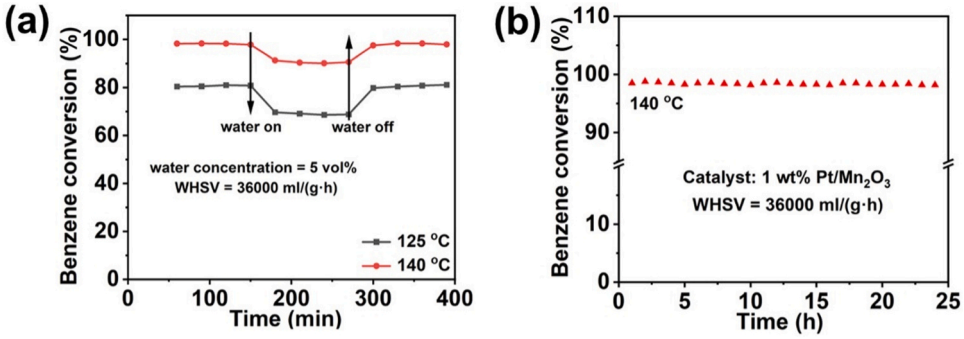

Fig. 5. Impact of water vapor on benzene oxidation at 125 °C and 140 °C (a) and the stability test at 140 °C (b) of 1 % Pt/Mn_2O_3 catalyst (Reprinted with permission from [182]).

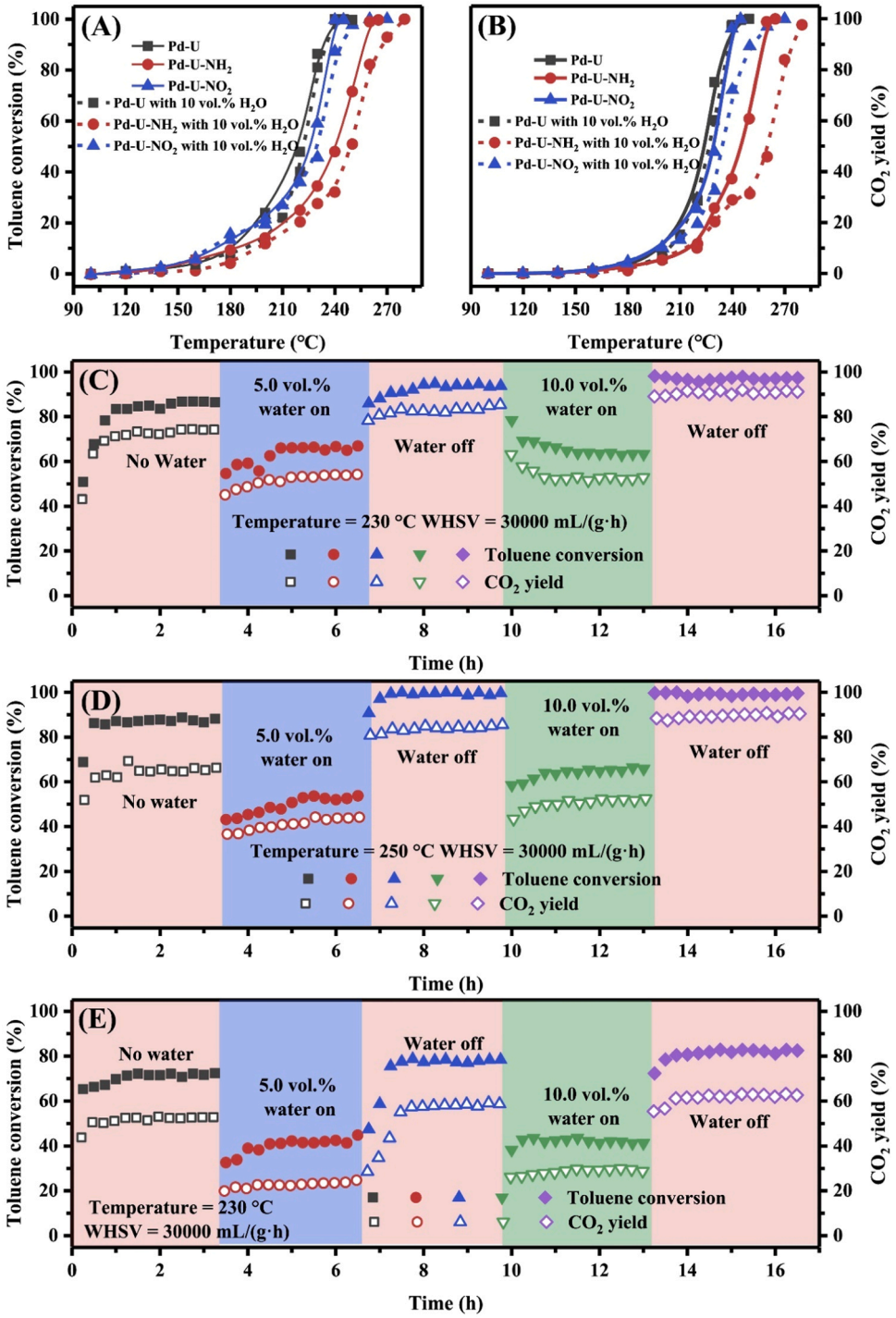

Fig. 6. Water-resistance of the supported Pd catalysts for toluene oxidation: temperature-dependent toluene conversion (A) and CO_2 yield (B) of the supported Pd catalysts in the absence and presence of water vapor; and the time-dependent water resistance of (C) Pd–U, (D) Pd–U–NH_2, and (E) Pd–U–NO_2 (Reprinted with permission from [83]).

particularly the synergistic effects of combining surface modification with operational adjustments, to develop catalysts that remain stable and efficient under the harsh conditions of industrial gas emissions.

6. Kinetics and mechanism of BTEX catalytic oxidation reactions

Kinetic model serves as a crucial tool in simulating the combustion/oxidation of BTEX and assessing the efficiency of BTEX degradation under diverse operational conditions. Three kinetic model categories are commonly used for BTEX catalytic abatement: the power law (PL) model, the Langmuir model, and Mars-van Krevelen (MvK) model. PL model seems inadequate for describing the chemistry of reactions, lacking a direct connection to the mechanisms involved. In contrast, the Langmuir model is constructed based on both Langmuir-Hinshelwood (L-H) mechanisms and Eley-Rideal (E-R). The Eley-rideal mechanism assumes the reaction to take place between gaseous BTEX and O_{ads}, rather than involving adsorbed BTEX compound [186]. The Langmuir-Hinshelwood mechanism assumes that oxygen adsorbed on the catalyst reacts with BTEX that is adsorbed, followed by a redox process [127]. The crucial step in this model is the surface reaction of the

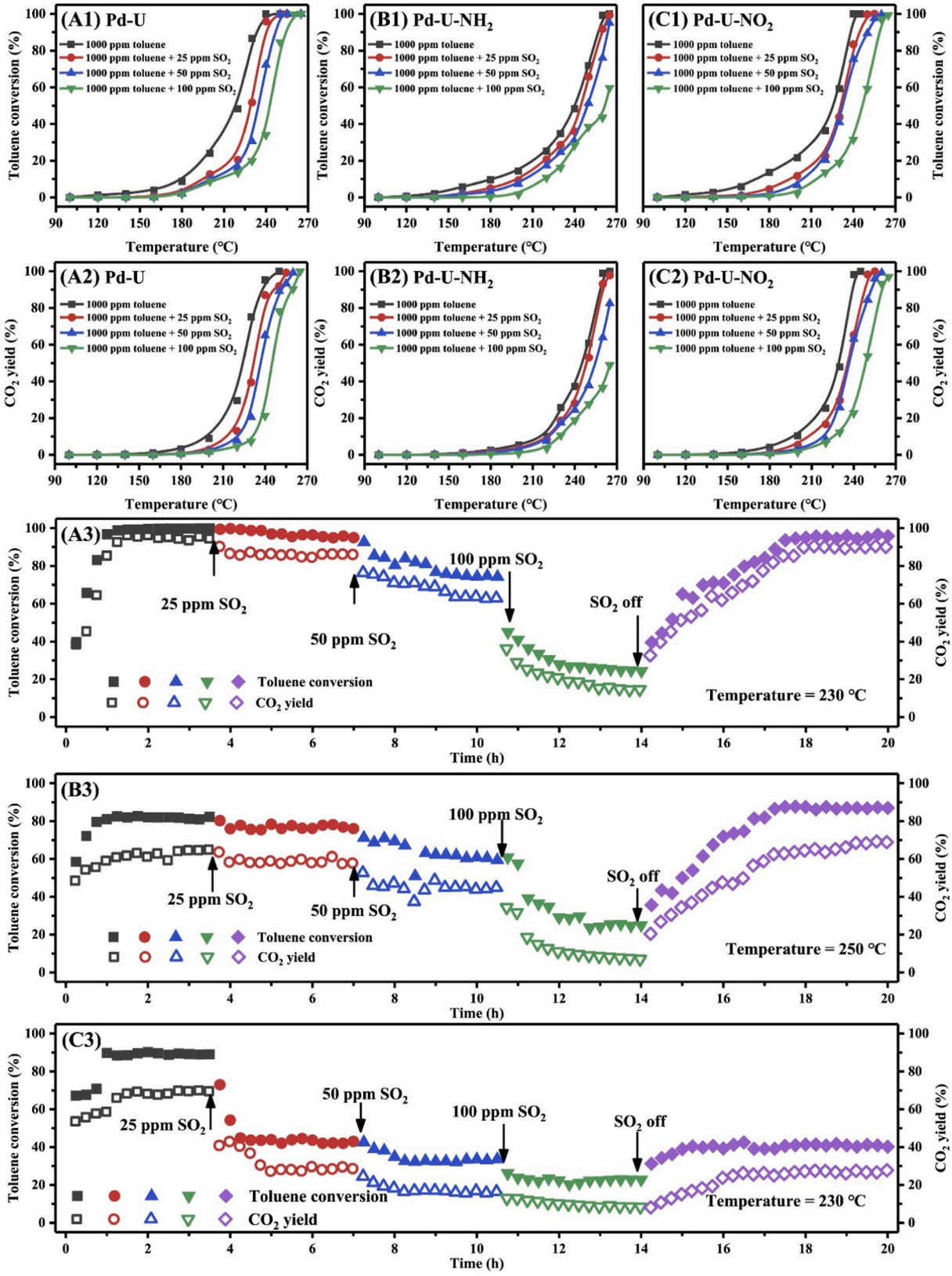

Fig. 7. Influence of SO_2 on the catalytic performance of the supported Pd catalysts for toluene oxidation; temperature-dependent toluene conversion (A1–C1), CO_2 yield (A2–C2), and temperature-dependent toluene conversion and CO_2 yield (A3–C3) in the presence of various concentrations of SO_2 over the supported Pd catalysts: (A) Pd–U, (B) Pd–U–NH_2, and (C) Pd–U–NO_2 (Reprinted with permission from [83]).

two adsorbed molecules on the active site, controlling the overall process [187]. On the other hand, the MvK model outlines a sequence where adsorbed BTEX initially reacts with oxygen within the catalyst, followed by metal oxide reduction. Subsequently, reoxidation of the reduced oxide takes place through the gas phase oxygen. Thus, this kind of mechanism is commonly referred to as the oxidation-reduction mechanism [188]. According to existing literature, Mars-Van Krevelen is more extensively employed in the study of BTEX degradation using various metal-based catalysts [34,37,39].

Comprehending the mechanism of reaction involved in BTEX catalytic degradation by diverse MOF-based/derived catalysts is crucial for developing high-performance, stable, and cost-effective MOF-based and MOF-derived catalysts. As previously noted, there exist diverse MOF-derivative catalysts for BTEX oxidation, and they may exhibit distinct mechanisms of reactions owing to variations in their compositions and structures. Such differences can influence the formation of various intermediate species during the oxidation process. MOF derivatives essentially refer to metal oxides, where the catalytic mechanism closely resembles the conventional catalytic process. The proposed mechanisms, as per existing literature, include the MVK, L–H, and E–R models [37,51].

Several mechanistic pathways have been proposed for BTEX degradation over different catalysts. Zhang and coworkers explored the mechanism of toluene oxidation using manganese cerium complex oxides derived from MOFs. Initially, toluene underwent adsorption and reacted with the catalyst's lattice oxygen and oxygen vacancies, leading to the conversion into CO_2 and H_2O. Eventually, oxygen vacancies were recharged through the activation of gaseous oxygen into lattice oxygen. Furthermore, their findings indicated that the H_2O present in the reaction system resulted in associative adsorption on oxygen vacancies. This process generated additional groups that are active or provided more active sites with surface oxygen, promoting the adsorbed oxygen conversion to lattice oxygen and accelerating toluene mineralization. This study affirmed that toluene degradation by metal oxide catalysts derived

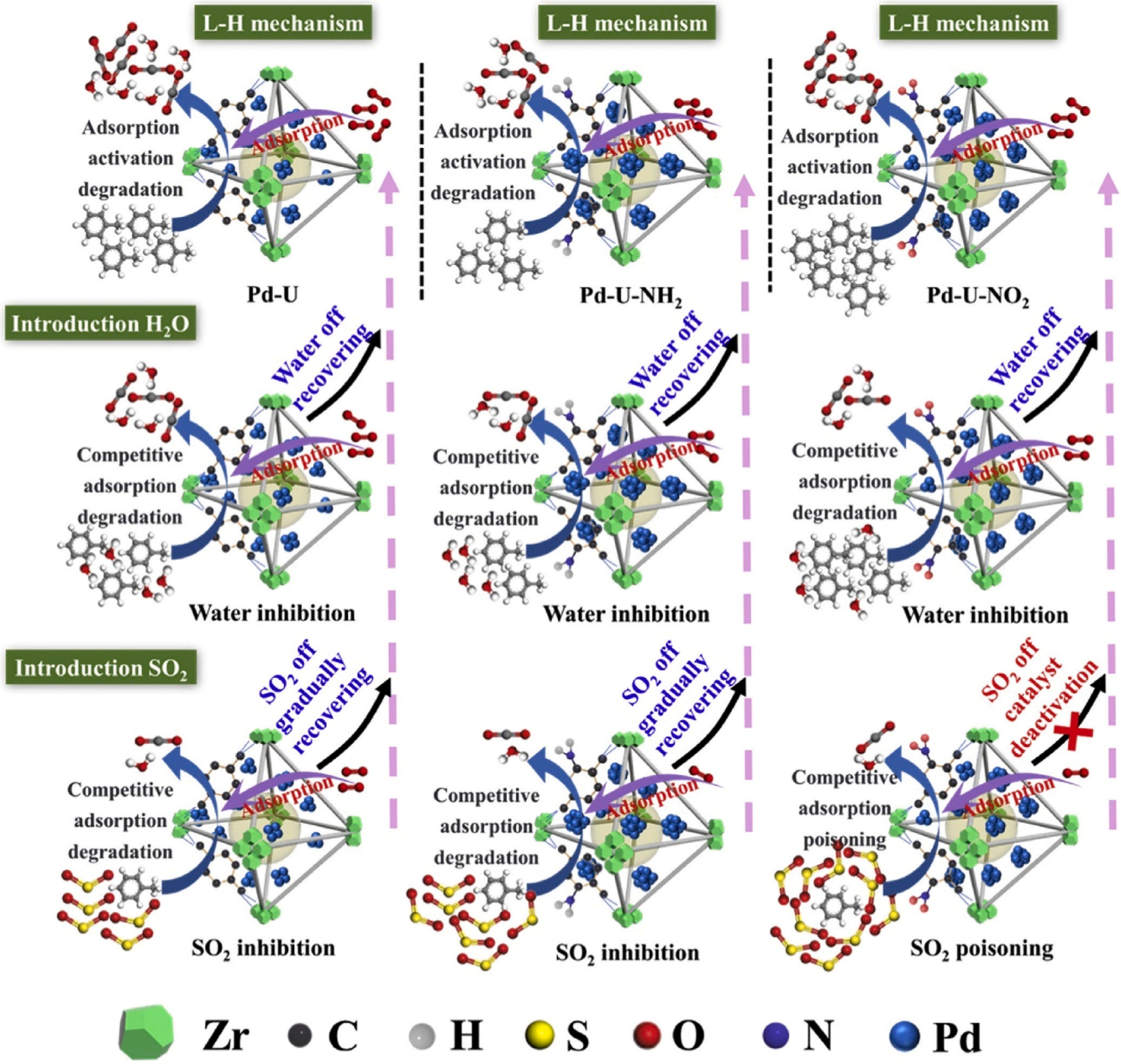

Fig. 8. Catalytic mechanism of toluene oxidation over the supported Pd catalysts (Reproduced with permission from [83]).

from MOFs adheres to the MvK model [109].

Bi et al. [83] presented the mechanism of reaction for the oxidation of toluene, using UiO-66 and its functional materials as supports for Pd. Their research involved calculating the degradation rate of toluene through toluene temperature-programmed surface reaction (TPSR) and temperature-programmed desorption (TPD), which affirmed the reaction between adsorbed oxygen and toluene. It was concluded that toluene degradation by loaded Pd catalysts followed the Langmuir-Hinshelwood mechanism as depicted in Fig. 8. In a separate investigation, it was demonstrated using DFT calculation that toluene oxidation on Pd-based catalysts follows the L-H reaction mechanism. The adsorbed oxygen activated by isolated Pd atom (Pd_1) reacted with adsorbed toluene on sub-nanometre Pd clusters (Pd_c) and Pd nanoparticles (Pd_n), leading to the mineralization of toluene into CO_2 and H_2O. This demonstrates the individual and synergistic role of various Pd species for toluene oxidation [76].

Xiao et al. [72] employed an in situ growth method within a MOF to synthesize Pt@Co_3O_4 catalysts, aiming to enhance toluene degradation, followed by an exploration of the mechanism of reaction. The in situ DRIFTS spectra of Pt@Co_3O_4 catalysts under oxygen-deficient conditions are presented in Fig. 9**(i)-(a)**. Evidently, intermediate species such as benzaldehyde, benzyl alcohol, maleic anhydride, and benzoate accumulated onto the Pt@Co_3O_4 catalyst surface over time. This implies significant involvement of both lattice oxygen and surface adsorbed oxygen in toluene degradation, even in the gaseous oxygen absence. In oxygen-rich conditions, similar spectra were observed in Pt@Co_3O_4 catalysts, indicating key intermediate species, analogous to Pt NPs@Co_3O_4 catalysts in oxygen-deficient conditions [Fig. 9(i)-(b)]. The rate-determining step, involving the opening of the ring or further benzoate oxidation to maleic anhydride, was apparent among the toluene degradation processes.

Despite the deficient active oxygen to facilitate the benzoate ring opening to maleic anhydride, the benzoate accumulation increased continuously over time, demonstrating a high capacity of lattice oxygen to move in toluene oxidation. EXAFS results affirmed that the active O_{latt} originated from the weak bond of Co–O. In contrast to oxygen-deficient conditions, maleic anhydride and benzoate continue to accumulate in oxygen-rich environment, illustrating the involvement of oxygen gas in the succeeding degradation process of toluene. Under oxygen-deficient environments, in situ DRIFTS revealed lattice oxygen consumption,

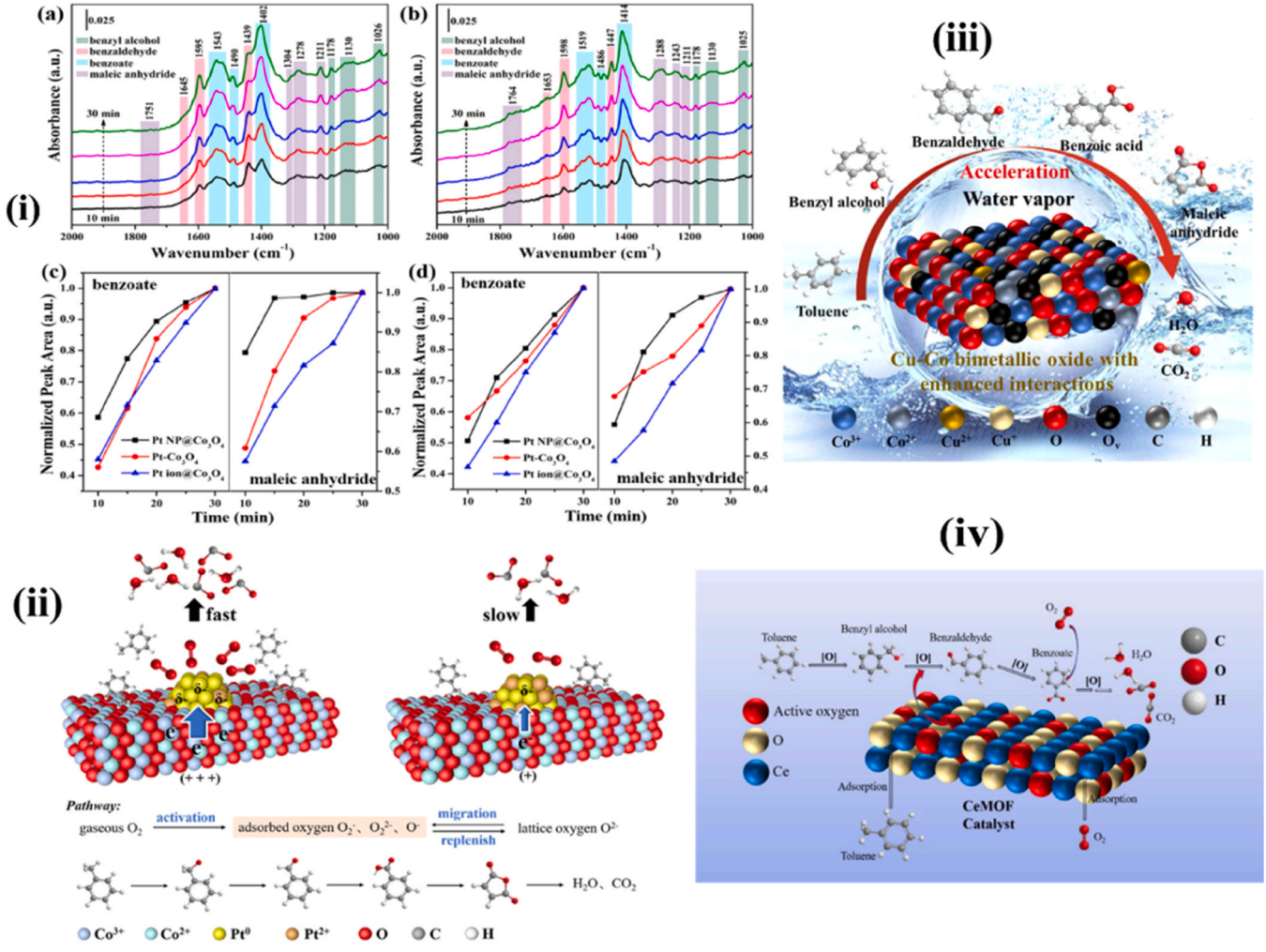

Fig. 9. (i) (a) In situ DRIFTS spectra of toluene adsorption as a function of time at 150 °C over the Pt NPs@Co_3O_4 catalyst (reaction condition: 1000 ppm toluene + N_2 balanced). (b) In situ DRIFTS spectra of toluene oxidation as a function of time at 170 °C over the Pt NPs@Co_3O_4 catalyst (reaction condition: 1000 ppm toluene + 20 % O_2 +N_2 balanced). (c) Plots of the formation amount of benzoate (left) and maleic anhydride (right) under oxygen-deficient conditions. (d) Plots of the formation amount of benzoate (left) and maleic anhydride (right) over Pt@ Co_3O_4 catalysts after the catalysts absorbed toluene for 30 min under oxygen-rich conditions (Reproduced with permission from [72]). (ii) (Top) Toluene degradation mechanism on Pt NPs@Co_3O_4 (left) and Pt ion@Co_3O_4 catalysts (right). (Bottom) The participation pathway of oxygen species in the process of the toluene reaction (Reproduced with permission from [72]). (iii) Possible oxidation pathway of toluene over $CuCoO_x$ in the existence of water vapors (Reproduced with permission from [168]. (iv) Mechanism for catalytic combustion of toluene over CeMOF (Reproduced with permission from [98]).

suggesting the activation of gaseous oxygen to recharge consumed O_{latt} in an oxygen-rich environment. The adequate introduction of active oxygen ensured succeeding toluene breakdown, leading to the intermediate species accumulation. Based on these observations, the proposed toluene degradation mechanism over Pt@Co_3O_4 catalysts is outlined in Fig. 9(ii).

Li et al. [98] suggested a reaction mechanism for toluene catalytic breakdown on CeMOF. Initially, toluene was adsorbed onto the surface of the catalyst, followed by oxidation to phenyl alcohol, benzaldehyde, and benzoic acid through the involvement of surface-active oxygen. Subsequently, ring opening of benzene took place, leading to further oxidation into other carboxylates. Then, intermediates are ultimately completely degraded to carbon dioxide and water (H_2O), after which they desorb from the catalyst surface (refer to Fig. 9(iv)). Similar reaction mechanism type was reported by Wu et al. [168] studying toluene degradation in the presence of water over $CuCoO_x$ catalysts derived from MOF. However, all intermediates are not the same as the one reported by Li et al. [98]. The first two intermediates (benzyl alcohol and benzaldehyde) are the same but the next intermediates are different. For Li et al. [98], the next one is benzoate but for Wu et al. [168], the following intermediates are benzoic acid and maleic acid (Fig. 9).

Noble metals supported on MOF-derived materials and transition metals supported on MOFs or derived from MOFs play a crucial role in impacting the mechanisms and efficiency of BTEX degradation reactions. By understanding the specific effects of these catalysts, we gain insights into their unique contribution to performance, selectivity, stability, and resistance to poisoning, all of which are critical for improving catalytic activity in practical applications.

Transition metal oxides like CeO_2, MnO_2, Fe_2O_3, and Co_3O_4 are frequently utilized owing to their variable oxidation states, which facilitate redox cycles and oxygen mobility essential for catalytic degradation reactions. When derived from or supported on metal-organic framework materials, they exhibit higher dispersion, unique porous structures, and greater surface area, which enhance their catalytic activity in BTEX degradation. MOF-derived transition metal oxides, especially those containing ceria, promote rapid oxygen storage and release, improving the degradation of BTEX compounds. For instance, Ce transitions between Ce^{3+} and Ce^{4+} states, facilitating oxygen transfer in redox cycle and enabling reactive oxygen species generation. This oxygen mobility is vital in the degradation of stable aromatic rings in BTEX, as it enables continuous catalytic performance by supplying active oxygen at the reaction sites [90]. Besides, transition metal oxides supported on MOF-derived materials often create reactive oxygen species such as superoxide and hydroxyl radicals, which are potent oxidants for degrading BTEX molecules. For instance, MnO_2, when supported on MOF-derived materials, is known to increase reactive oxygen species generation through multiple oxidation states ($Mn^{2+}/Mn^{3+}/Mn^{4+}$), facilitating BTEX decomposition by attacking the aromatic rings more effectively [105]. Furthermore, MOF-derived transition metal oxides often exhibit improved electronic properties owing to their structural modification during the pyrolysis of metal-organic frameworks. For example, Co_3O_4 derived from MOF can have enhanced electron density around the active sites, which facilitates electron transfer during the degradation process. This enhanced electron transfer boosts the activation of molecular oxygen and improves the BTEX degradation rate [106].

Noble metals such as Pt, Pd, Au, and Ru are known for their high catalytic efficiency in oxidation reactions, especially for VOCs like BTEX. When supported on MOF-derived materials, noble metals exhibit improved dispersion, reduced agglomeration, and stabilized active sites owing to the high surface area and porosity of MOF-derived materials. For example, Pt and Pd nanoparticles supported on MOF-derived materials can dissociate molecular oxygen into atomic oxygen, which readily participates in degradation reactions with BTEX. This activation of molecular oxygen is critical in initiating degradation pathways at lower temperatures, making these catalysts effective for low-temperature BTEX degradation [57,58]. Moreover, noble metals promote the "spillover effect", where the activated oxygen species migrate from noble metal sites to adjacent metal oxide support sites, increasing the degradation activity over the entire surface of the catalyst. In Pt-supported MOF-derived materials, for example, atomic oxygen created at Pt sites can spill over to nearby transition metal oxide sites, generating additional active centers for BTEX oxidation. This effect enhances the overall efficiency and use of oxygen on the surface of the catalyst, leading to more complete degradation of BTEX [81]. Furthermore, when noble metals are supported on MOF-derived oxides, synergistic interactions increase catalytic activity. For instance, Pt@CeO_2 derived from MOF exhibit improved catalytic performance owing to the electronic interaction between CeO_2 and Pt, which facilitates electron transfer and stabilizes active oxygen species. These synergistic interactions also enhance the redox cycles of Ce, which in turn, reformates the catalytic sites and sustains the oxidation performance [56].

The presence of transition metal oxides and noble metals in MOF-derived materials influences various oxidation mechanisms such as MvK, L-H, and E-R mechanisms. Many MOF-derived transition metal oxides, like CeO_2 and MnO_2, operate through the MvK mechanism, where lattice oxygen directly participates in BTEX degradation. In this process, lattice oxygen from transition metal oxide is consumed during the degradation reaction and subsequently replenished by molecular oxygen from the gas phase. Noble metals, such as Pt or Pd, enhance this mechanism by accelerating the reformation of lattice oxygen, which improves the overall turnover rate for BTEX degradation. Few MOF-derived transition metal oxides and noble metals operate through the L-H and E-R mechanisms.

Currently, investigations into catalytic mechanisms have predominantly centered around noble metal MOF derivative catalysts and transition metal oxides derived from MOF, with limited attention given to the exploration of the influence of MOFs and their derived structures on the BTEX oxidation reaction mechanism. BTEX compounds investigated were single, and there was a scarcity of research on multiple combined components and diverse influencing factors. Addressing these gaps is an urgent concern for future studies aimed at developing catalysts with greater potential.

Recent studies have used kinetic modeling and simulation data to predict and optimize catalytic performance in BTEX oxidation reactions. For instance, the Mars-van Krevelen model has been extensively employed to simulate the dynamic behavior of catalytic systems, providing insights into reaction rates and the effect of operational parameters. Simulations have shown that the efficiency of BTEX oxidation is significantly influenced by the oxygen vacancy concentration and the reducibility of the metal oxide lattice. Incorporating these kinetic models into catalyst design enables the fine-tuning of catalytic properties to enhance performance under real-world conditions.

Deploying transition metal oxides derived from MOFs or supported on MOFs and noble metals supported on MOF-derived materials in large-scale operations for BTEX degradation involves various key challenges. Although these catalysts are promising in laboratory settings owing to their high efficiency, stability, and selectivity, scaling up presents technical, economic, and operational difficulties that must be addressed for commercial applications [61]. The main challenges include the cost and availability of raw materials especially for noble metals and precursors for MOF synthesis; complex and energy-intensive synthesis processes for transition metal oxide, noble metal doping, and MOF synthesis; structural stability and longevity under real-world conditions due to thermal stability and inhibitors; optimization of catalyst performance for practical reactor conditions especially mass transfer limitations and manipulating the catalyst activation mechanisms; Operational and maintenance challenges for mechanical stability and catalyst regeneration; environmental and safety concerns related to waste management and safety in high-temperature operations; scalability and reproducibility of catalyst properties such as uniformity of active sites and reproducibility in large-scale production then limited

understanding of long-term catalyst behavior [61].

Addressing these challenges will require advances in catalyst preparation, structural stabilization, cost reduction, and optimization for practical reactor conditions. Innovations in scalable green synthesis techniques, developing cost-effective alternatives to noble metals, and an improved understanding of long-term catalyst behavior are critical steps toward successfully deploying MOF-derived materials for large-scale BTEX degradation. These advancements will help bridge the gap between promising lab results and real-world industrial applications.

7. Conclusions

The advancements in MOF-based and MOF-derived catalysts have significantly contributed to the efficient oxidation of BTEX pollutants. Through a systematic analysis of catalyst structures, compositional modifications, and catalytic mechanisms, this review highlights the pivotal role of MOF-derived materials in achieving high conversion efficiencies, improved selectivity, and enhanced stability under varied operational conditions. Notably, noble metal-supported MOF catalysts exhibit superior low-temperature catalytic efficiency, often achieving over 90 % BTEX conversion at temperatures as low as 180 °C, while transition metal oxides and bimetallic catalysts demonstrate remarkable stability and resistance to deactivation.

Mechanistic insights into BTEX degradation pathways, including the Mars-Van Krevelen, Langmuir-Hinshelwood, and Eley-Rideal models, underscore the importance of oxygen vacancy formation and active site exposure in enhancing catalytic performance. The presence of highly dispersed noble metals, strong metal-support interactions, and tailored electronic effects has been instrumental in optimizing catalyst performance. Additionally, the review identifies the critical challenges facing MOF-based catalysts, such as deactivation due to SO_2 poisoning, water vapor interference, and structural instability under high-temperature conditions.

Future research should prioritize the development of highly durable, cost-effective, and scalable MOF-derived catalysts by exploring single-atom catalysts, multi-metallic frameworks, and innovative regeneration strategies. Furthermore, computational modeling and in-situ characterization techniques should be employed to gain deeper insights into catalyst structure-activity relationships. Addressing these challenges will not only enhance the practical application of MOF-derived catalysts in industrial-scale BTEX oxidation but also contribute to the advancement of sustainable air pollution control technologies.

By bridging fundamental research with industrial applicability, MOF-based catalysts hold immense promise in revolutionizing VOC abatement strategies, making significant contributions toward cleaner air and environmental sustainability.

8. Challenges and future perspectives

Understanding MOF-derived catalysts' role in BTEX oxidation is a nascent field facing significant challenges. Moving forward, key areas of focus include mitigating catalyst deactivation and poisoning caused by adsorption of SO_x, NO_x, CO, and H_2O in industrial exhausts. A deeper grasp of these mechanisms is vital to design robust, poison-resistant catalysts. Additionally, while MOF-based catalysts improve gaseous pollutant adsorption and diffusion, their behavior in complex BTEX exhausts is poorly understood. The diverse interactions between BTEX compounds and different MOF structures remain largely unexplored, hindering effective multi-component gas treatment. Understanding these interactions is critical for assessing MOF catalysts' viability under real operational conditions. Regenerating catalysts is crucial for cost-effectiveness, but existing methods like high-temperature decoking may compromise MOF catalyst integrity and activity. Thus, there is a need for tailored regeneration processes. Given MOFs' pivotal role in BTEX oxidation, understanding how regeneration affects catalyst structure and activity is paramount. In summary, advancing MOF-derived catalyst research necessitates addressing catalyst poisoning, multi-component gas interactions, and tailored regeneration methods. This holistic approach is vital for realizing efficient and sustainable BTEX treatment in industrial settings.

CRediT authorship contribution statement

Li Jianrong: Writing – review & editing, Software, Resources, Investigation. **Chen George Zheng:** Writing – review & editing, Supervision, Project administration. **He Jun:** Writing – review & editing, Supervision, Resources, Project administration, Funding acquisition, Conceptualization. **Yusuf Abubakar:** Writing – review & editing, Supervision, Methodology, Formal analysis, Conceptualization. **Xiao Zhiyu:** Writing – review & editing, Investigation, Conceptualization. **Wang Zongshuang:** Writing – review & editing, Resources, Investigation. **Murindababisha David:** Writing – original draft, Methodology, Investigation, Data curation, Conceptualization.

Declaration of Competing Interest

The authors declare the following financial interests/personal relationships which may be considered as potential competing interests: Jun He reports financial support was provided by Ningbo Science and Technology Bureau. If there are other authors, they declare that they have no known competing financial interests or personal relationships that could have appeared to influence the work reported in this paper.

Acknowledgements

This work was jointly sponsored by the Ningbo Science and Technology Innovation Key Project (2022Z028), Ningbo Natural Science Foundation Grant (2023J024), Ningbo Commonweal Key Research Program (2023S038) and Ningbo Key Technology Breakthrough Scheme Projects under Yongjiang Science and Innovation 2035 (2024Z237, 2024Z251).

Data availability

Data will be made available on request.

References

[1] A.H. Khoshakhlagh, S. Yazdanirad, M. Mousavi, A. Gruszecka-Kosowska, M. Shahriyari, H. Rajabi-Vardanjani, Summer and winter variations of BTEX concentrations in an oil refinery complex and health risk assessment based on Monte-Carlo simulations, Sci. Rep. 13 (2023) 1–15.
[2] A. Wongbunmak, S. Khiawjan, M. Suphantharika, T. Pongtharangkul, BTEX biodegradation by Bacillus amyloliquefaciens subsp. plantarum W1 and its proposed BTEX biodegradation pathways, Sci. Rep. 10 (2020) 1–13.
[3] Y. Lee, Y. Lee, C.O. Jeon, Biodegradation of naphthalene, BTEX, and aliphatic hydrocarbons by Paraburkholderia aromaticivorans BN5 isolated from petroleum-contaminated soil, Sci. Rep. 9 (2019) 24–30.
[4] M. Dehghani, A. Abbasi, Z. Taherzadeh, S. Dehghani, Exposure assessment of wastewater treatment plant employees to BTEX: a biological monitoring approach, Sci. Rep. 12 (2022) 1–10.
[5] E. Durmusoglu, F. Taspinar, A. Karademir, Health risk assessment of BTEX emissions in the landfill environment, J. Hazard. Mater. 176 (2010) 870–877.
[6] D.O. Njobuenwu, S.A. Amadi, P.C. Ukpaka, Dissolution rate of BTEX contaminants in water, Can. J. Chem. Eng. 83 (2005) 985–989.
[7] F. Golkhorshidi, A. Sorooshian, A.J. Jafari, A.N. Baghani, M. Kermani, R. R. Kalantary, Q. Ashournejad, M. Delikhoon, On the nature and health impacts of BTEX in a populated middle eastern city: Tehran, Iran, Atmos. Pollut. Res. 10 (2019) 921–930.
[8] M.T. Latif, H.H. Abd Hamid, F. Ahamad, M.F. Khan, M.S. Mohd Nadzir, M. Othman, M. Sahani, M.I. Abdul Wahab, N. Mohamad, R. Uning, S.C. Poh, M. F. Fadzil, J. Sentian, N.M. Tahir, BTEX compositions and its potential health impacts in Malaysia, Chemosphere 237 (2019) 1–12.
[9] B. Yu, Z. Yuan, Z. Yu, F. Xue-song, BTEX in the environment: an update on sources, fate, distribution, pretreatment, analysis, and removal techniques, Chem. Eng. J. 435 (2022) 134825.
[10] A. Masih, A.S. Lall, A. Taneja, R. Singhvi, Exposure profiles, seasonal variation and health risk assessment of BTEX in indoor air of homes at different

microenvironments of a terai province of northern India, Chemosphere 176 (2017) 8–17.
[11] S. Wang, W. Wei, D. Li, K. Aunan, J. Hao, Air pollutants in rural homes in Guizhou, China - concentrations, speciation, and size distribution, Atmos. Environ. 44 (2010) 4575–4581.
[12] K. Liu, C. Zhang, Y. Cheng, C. Liu, H. Zhang, G. Zhang, X. Sun, Y. Mu, Serious BTEX pollution in rural area of the North China Plain during winter season, J. Environ. Sci. (China). 30 (2015) 186–190.
[13] H.L. Wang, C.H. Chen, Q. Wang, C. Huang, L.Y. Su, H.Y. Huang, S.R. Lou, M. Zhou, L. Li, L.P. Qiao, Y.H. Wang, Chemical loss of volatile organic compounds and its impact on the source analysis through a two-year continuous measurement, Atmos. Environ. 80 (2013) 488–498.
[14] F.V. Hackbarth, V.J.P. Vilar, G.B. De Souza, S.M.A.G.U. de Souza, A.A.U. de Souza, Benzene, toluene and o-xylene (BTX) removal from aqueous solutions through adsorptive processes, Adsorption 20 (2014) 577–590.
[15] H. Amini, V. Hosseini, C. Schindler, H. Hassankhany, M. Yunesian, S. B. Henderson, N. Künzli, Spatiotemporal description of BTEX volatile organic compounds in a Middle Eastern megacity: Tehran Study of Exposure Prediction for Environmental Health Research (Tehran SEPEHR), Environ. Pollut. 226 (2017) 219–229.
[16] M. Guillerm, A. Couvert, A. Amrane, E. Norrant, N. Lesage, É . Dumont, Absorption of toluene in silicone oil: effect of the solvent viscosity on hydrodynamics and mass transfer, Chem. Eng. Res. Des. 109 (2016) 32–40.
[17] S. Lu, Q. Liu, R. Han, J. Shi, M. Guo, C. Song, N. Ji, X. Lu, D. Ma, Core-shell structured Y zeolite/hydrophobic organic polymer with improved toluene adsorption capacity under dry and wet conditions, Chem. Eng. J. 409 (2021) 128194.
[18] M. Woellner, S. Hausdorf, N. Klein, P. Mueller, M.W. Smith, S. Kaskel, Adsorption and detection of hazardous trace gases by metal–organic frameworks, Adv. Mater. 30 (2018) 1–27.
[19] I. García-Peña, I. Ortiz, S. Hernández, S. Revah, Biofiltration of BTEX by the fungus Paecilomyces variotii, Int. Biodeterior. Biodegrad. 62 (2008) 442–447.
[20] S. Salvador, J.M. Commandré, Y. Kara, Thermal recuperative incineration of VOCs: CFD modelling and experimental validation, Appl. Therm. Eng. 26 (2006) 2355–2366.
[21] X. Rong, Q. Cao, Y. Gao, T. Luan, Y. Li, Q. Man, Z. Zhang, B. Chen, Synergistic catalytic performance of toluene degradation based on non-thermal plasma and Mn/Ce-based bimetal-organic frameworks, Molecules 27 (2022) 7363.
[22] Z. Huang, H. Li, X. Zhang, Y. Mao, Y. Wu, W. Liu, H. Gao, M. Zhang, Z. Song, Catalytic oxidation of toluene by manganese oxides: effect of K^+ doping on oxygen vacancy, J. Environ. Sci. 142 (2023) 43–56.
[23] L. Cheng, Y. Li, J. Fan, M. Xie, X. Liu, P. Sun, X. Dong, High efficiency photothermal synergistic degradation of toluene achieved through the utilization of a nickel foam loaded Pt-CeO_2 monolithic catalyst, Sep. Purif. Technol. 333 (2024) 125742.
[24] E. Dumont, G. Darracq, A. Couvert, C. Couriol, A. Amrane, D. Thomas, Y. Andrès, P. Le Cloirec, VOC absorption in a countercurrent packed-bed column using water/silicone oil mixtures: influence of silicone oil volume fraction, Chem. Eng. J. 168 (2011) 241–248.
[25] P. Dwivedi, V. Gaur, A. Sharma, N. Verma, Comparative study of removal of volatile organic compounds by cryogenic condensation and adsorption by activated carbon fiber, Sep. Purif. Technol. 39 (2004) 23–37.
[26] C. Yang, G. Miao, Y. Pi, Q. Xia, J. Wu, Z. Li, J. Xiao, Abatement of various types of VOCs by adsorption/catalytic oxidation: a review, Chem. Eng. J. 370 (2019) 1128–1153.
[27] K. Vellingiri, P. Kumar, A. Deep, K.H. Kim, Metal-organic frameworks for the adsorption of gaseous toluene under ambient temperature and pressure, Chem. Eng. J. 307 (2017) 1116–1126.
[28] S. Wang, H.M. Ang, M.O. Tade, Volatile organic compounds in indoor environment and photocatalytic oxidation: state of the art, Environ. Int. 33 (2007) 694–705.
[29] Z. Shayegan, C.S. Lee, F. Haghighat, TiO_2 photocatalyst for removal of volatile organic compounds in gas phase – a review, Chem. Eng. J. 334 (2018) 2408–2439.
[30] X. Zhang, X. Lv, X. Shi, Y. Yang, Y. Yang, Enhanced hydrophobic UiO-66 (University of Oslo 66) metal-organic framework with high capacity and selectivity for toluene capture from high humid air, J. Colloid Interface Sci. 539 (2019) 152–160.
[31] Y. Zheng, Q. Liu, C. Shan, Y. Su, K. Fu, S. Lu, R. Han, C. Song, N. Ji, D. Ma, Defective ultrafine MnO_x nanoparticles confined within a carbon matrix for low-temperature oxidation of volatile organic compounds, Environ. Sci. Technol. 55 (2021) 5403–5411.
[32] J. Zhang, X. Xu, S. Zhao, X. Meng, F.S. Xiao, Recent advances of zeolites in catalytic oxidations of volatile organic compounds, Catal. Today 410 (2023) 56–67.
[33] L. Zhang, L. Xue, B. Lin, Q. Zhao, S. Wan, Y. Wang, H. Jia, H. Xiong, Noble metal single-atom catalysts for the catalytic oxidation of volatile organic compounds, ChemSusChem 15 (2022) e202102494.
[34] D. Murindababisha, A. Yusuf, Y. Sun, C. Wang, Y. Ren, J. Lv, H. Xiao, Current progress on catalytic oxidation of toluene: a review, Environ. Sci. Pollut. Res. 28 (2021) 62030–62060.
[35] Y. Luo, Y. Zheng, J. Zuo, X. Feng, X. Wang, T. Zhang, K. Zhang, L. Jiang, Insights into the high performance of Mn-Co oxides derived from metal-organic frameworks for total toluene oxidation, J. Hazard. Mater. 349 (2018) 119–127.
[36] Y. Xia, H. Dai, H. Jiang, L. Zhang, Three-dimensional ordered mesoporous cobalt oxides: highly active catalysts for the oxidation of toluene and methanol, Catal. Commun. 11 (2010) 1171–1175.
[37] M. Hao, M. Qiu, H. Yang, B. Hu, X. Wang, Recent advances on preparation and environmental applications of MOF-derived carbons in catalysis, Sci. Total Environ. 760 (2021) 143333.
[38] R. Rao, S. Ma, B. Gao, F. Bi, Y. Chen, Y. Yang, N. Liu, M. Wu, X. Zhang, Recent advances of metal-organic framework-based and derivative materials in the heterogeneous catalytic removal of volatile organic compounds, J. Colloid Interface Sci. 636 (2023) 55–72.
[39] D. Wang, C. Yuan, C. Yang, P. Wang, Y. Zhan, N. Guo, L. Jiang, Z. Wang, Z. Wang, Recent advances in catalytic removal volatile organic compounds over metal–organic framework–derived catalysts: a review, Sep. Purif. Technol. 326 (2023) 124765.
[40] L. Jiao, H.L. Jiang, Metal-organic framework-based single-atom catalysts for energy applications, Chem 5 (2019) 786–804.
[41] X. Han, W. Chen, X. Han, Y. Tan, D. Sun, Nitrogen-rich MOF derived porous Co_3O_4/N–C composites with superior performance in lithium- ion batteries, J. Mater. Chem. A 4 (2016) 13040–13045.
[42] X. Zhao, H. Yang, P. Jing, W. Shi, G. Yang, P. Cheng, A metal-organic framework approach toward highly nitrogen-doped graphitic carbon as a metal-free photocatalyst for hydrogen evolution, Small 13 (2016) 1–6.
[43] S. Wei, A. Li, J. Liu, Z. Li, W. Chen, Y. Gong, Q. Zhang, W. Cheong, Y. Wang, L. Zheng, H. Xiao, C. Chen, D. Wang, Direct observation of noble metal nanoparticles transforming to thermally stable single atoms, Nat. Nanotechnol. 13 (2018) 856–861.
[44] S. Osman, R.A. Senthil, J. Pan, W. Li, Highly activated porous carbon with 3D microspherical structure and hierarchical pores as greatly enhanced cathode material for high- performance supercapacitors, J. Power Sources 391 (2018) 162–169.
[45] L. Zhu, D. Shen, K. Hong, A critical review on VOCs adsorption by different porous materials: species, mechanisms and modification methods, J. Hazard. Mater. 389 (2020) 122102.
[46] A. Fernandes, P. Mako, J. Ali, G. Boczkaj, Integrated photocatalytic advanced oxidation system (TiO_2/UV/O_3/H_2O_2) for degradation of volatile organic compounds, Sep. Purif. Technol. 224 (2019) 1–14.
[47] R.R. Salunkhe, Y.V. Kaneti, Y. Yamauchi, Metal−organic framework-derived nanoporous metal oxides toward supercapacitor applications: progress and prospects, ACS Nano 11 (2017) 5293–5308.
[48] K. Vellingiri, V. Choudhary, S. Kumar, L. Philip, Sorptive removal versus catalytic degradation of aqueous BTEX: a comprehensive review from the perspective of life-cycle assessment, Environ. Sci. Water Res. Technol. 8 (2022) 1359–1390.
[49] P. Behera, S. Subudhi, S.P. Tripathy, K. Parida, MOF derived nano-materials: a recent progress in strategic fabrication, characterization and mechanistic insight towards divergent photocatalytic applications, Coord. Chem. Rev. 456 (2022) 214392.
[50] M. Tomatis, H. Xu, J. He, X. Zhang, Recent development of catalysts for removal of volatile organic compounds in flue gas by combustion: a review, J. Chem. 2016 (2016) 8324826.
[51] D.P. Bhattarai, B. Pant, J. Acharya, M. Park, G.P. Ojha, Recent progress in metal–organic framework-derived nanostructures in the removal of volatile organic compounds, Molecules 26 (2021) 1–18.
[52] J. Deng, S. He, S. Xie, H. Yang, Y. Liu, G. Guo, H. Dai, Ultralow loading of silver nanoparticles on Mn_2O_3 nanowires derived with molten salts: a high-efficiency catalyst for the oxidative removal of toluene, Environ. Sci. Technol. 49 (2015) 11089–11095.
[53] X. Li, G. He, J. Ma, X. Shao, Y. Chen, H. He, Boosting the dispersity of metallic Ag nanoparticles and ozone decomposition performance of Ag-Mn catalysts via manganese vacancy-dependent metal-support interactions, Environ. Sci. Technol. 55 (2021) 16143.
[54] N. Guo, J. Zhang, L. Jiang, D. Wang, Z. Wang, Highly efficient and selective Ru and Ce modified ZSM-5 catalysts for catalytic oxidation of toluene, Colloids Surf. A Physicochem. Eng. Asp. 651 (2022) 129709.
[55] X. Han, X. Chen, Y. Zou, S. Zhang, Electronic state regulation of supported Pt catalysts dictates selectivity of imines/secondary amines from the cascade transformation of nitroarenes and aldehydes, Appl. Catal. B Environ. 268 (2020) 118451.
[56] R. Peng, S. Li, X. Sun, Q. Ren, L. Chen, M. Fu, J. Wu, D. Ye, Size effect of Pt nanoparticles on the catalytic oxidation of toluene over Pt/CeO_2 catalysts, Appl. Catal. B Environ. 220 (2018) 462–470.
[57] H. Sun, X. Yu, Y. Guo, J. Deng, M. Ge, Achieving efficient toluene oxidation over metal–organic framework-derived Pt/CeO_2-Co_3O_4 catalyst, Appl. Surf. Sci. 591 (2022) 153225.
[58] F. Bi, S. Ma, B. Gao, B. Liu, Y. Huang, R. Qiao, X. Zhang, Boosting toluene deep oxidation by tuning metal-support interaction in MOF-derived Pd@ZrO_2 catalysts: The role of interfacial interaction between Pd and ZrO_2, Fuel 357 (2024) 129833.
[59] F. Bi, X. Zhang, J. Chen, Y. Yang, Y. Wang, Excellent catalytic activity and water resistance of UiO-66-supported highly dispersed Pd nanoparticles for toluene catalytic oxidation, Appl. Catal. B Environ. 269 (2020) 118767.
[60] J. Li, Z. Xu, T. Wang, X. Xie, D. Li, J. Wang, H. Huang, Z. Ao, A versatile route to fabricate Metal/UiO-66 (Metal = Pt, Pd, Ru) with high activity and stability for the catalytic oxidation of various volatile organic compounds, Chem. Eng. J. 448 (2022) 136900.

[61] A.M. Wright, M.T. Kapelewski, S. Marx, O.K. Farha, W. Morris, Transitioning metal–organic frameworks from the laboratory to market through applied research, Nat. Mater. (2024) 1–10.
[62] M. Lammert, C. Glißmann, H. Reinsch, N. Stock, Synthesis and characterization of new Ce(IV)-MOFs exhibiting various framework topologies, Cryst. Growth Des. 17 (2017) 1125–1131.
[63] Y. Wang, F. Bi, Y. Wang, M. Jia, X. Tao, Y. Jin, X. Zhang, MOF-derived CeO_2 supported Ag catalysts for toluene oxidation: the effect of synthesis method, Mol. Catal. 515 (2021) 111922.
[64] Y. Liu, G. Chen, J. Chen, H. Niu, Excellent catalytic performance of Ce–MOF with abundant oxygen vacancies supported noble metal Pt in the oxidation of toluene, Catalysts 12 (2022) 775.
[65] J. Zheng, Z. Wang, Z. Chen, S. Zuo, Mechanism of CeO_2 synthesized by thermal decomposition of Ce-MOF and its performance of benzene catalytic combustion, J. Rare Earths 39 (2021) 790–796.
[66] S. Hyok Ri, F. Bi, A. Guan, X. Zhang, Manganese-cerium composite oxide pyrolyzed from metal organic framework supporting palladium nanoparticles for efficient toluene oxidation, J. Colloid Interface Sci. 586 (2021) 836–846.
[67] J. Zhong, Y. Zeng, M. Zhang, W. Feng, D. Xiao, J. Wu, P. Chen, M. Fu, D. Ye, Toluene oxidation process and proper mechanism over Co_3O_4 nanotubes: Investigation through in-situ DRIFTS combined with PTR-TOF-MS and quasi in-situ XPS, Chem. Eng. J. 397 (2020) 125375.
[68] Y. Liu, G. Wang, C. Xu, W. Wang, Fabrication of Co_3O_4 nanorods by calcination of precursor powders prepared in a novel inverse microemulsion, Chem. Commun. 2 (2002) 1486–1487.
[69] Y. Zhang, Y. Chen, T. Wang, J. Zhou, Y. Zhao, Synthesis and magnetic properties of nanoporous Co_3O_4 nanoflowers, Microporous Mesoporous Mater. 114 (2008) 257–261.
[70] X. Liu, J. Wang, J. Zeng, X. Wang, T. Zhu, Catalytic oxidation of toluene over a porous Co_3O_4-supported ruthenium catalyst, RSC Adv. 5 (2015) 52066–52071.
[71] J. Li, W. Li, G. Liu, Y. Deng, J. Yang, Y. Chen, Tricobalt tetraoxide-supported palladium catalyst derived from metal organic frameworks for complete benzene oxidation, Catal. Lett. 146 (2016) 1300–1308.
[72] M. Xiao, X. Yu, Y. Guo, M. Ge, Boosting toluene combustion by tuning electronic metal–support interactions in In situ grown Pt@Co_3O_4 catalysts, Environ. Sci. Technol. 56 (2022) 1376–1385.
[73] A.E. Platero-Prats, A. Mavrandonakis, L.C. Gallington, Y. Liu, J.T. Hupp, O. K. Farha, C.J. Cramer, K.W. Chapman, Structural transitions of the metal-oxide nodes within metal-organic frameworks: on the local structures of NU-1000 and UiO-66, J. Am. Chem. Soc. 138 (2016) 4178–4185.
[74] Y.X. Li, Z.Y. Wei, L. Liu, M.L. Gao, Z.B. Han, Ag nanoparticles supported on UiO-66 for selective oxidation of styrene, Inorg. Chem. Commun. 88 (2018) 47–50.
[75] X. Zhang, L. Song, F. Bi, D. Zhang, Y. Wang, L. Cui, Catalytic oxidation of toluene using a facile synthesized Ag nanoparticle supported on UiO-66 derivative, J. Colloid Interface Sci. 571 (2020) 38–47.
[76] X. Zhang, F. Bi, Z. Zhao, Y. Yang, Y. Li, L. Song, N. Liu, J. Xu, L. Cui, Boosting toluene oxidation by the regulation of Pd species on UiO-66: Synergistic effect of Pd species, J. Catal. 413 (2022) 59–75.
[77] Q. Guan, B. Wang, X. Chai, J. Liu, J. Gu, P. Ning, Comparison of Pd-UiO-66 and Pd-UiO-66-NH_2 catalysts performance for phenol hydrogenation in aqueous medium, Fuel 205 (2017) 130–141.
[78] Y. Yang, D. Zhang, W. Ji, F. Bi, L. Song, X. Zhang, Uniform platinum nanoparticles loaded on Universitetet i Oslo-66 (UiO-66): active and stable catalysts for gas toluene combustion, J. Colloid Interface Sci. 606 (2022) 1811–1822.
[79] S. Li, Y. Lin, D. Wang, C. Zhang, Z. Wang, X. Li, Polyhedral cobalt oxide supported Pt nanoparticles with enhanced performance for toluene catalytic oxidation, Chemosphere 263 (2021) 127870.
[80] F. Bi, Z. Zhao, Y. Yang, W. Gao, N. Liu, Y. Huang, X. Zhang, Chlorine-coordinated Pd single atom enhanced the chlorine resistance for volatile organic compound degradation: mechanism study, Environ. Sci. Technol. 56 (2022) 17321–17330.
[81] L. Li, Y. Jin, M. Wei, R. Wang, Z. Fei, Pt-modified 3D $MnCoO_x$ nanocages as effective catalysts for toluene oxidation, J. Alloy. Compd. 955 (2023) 170257.
[82] X. Chen, X. Chen, S. Cai, J. Chen, W. Xu, H. Jia, J. Chen, Catalytic combustion of toluene over mesoporous Cr_2O_3-supported platinum catalysts prepared by in situ pyrolysis of MOFs, Chem. Eng. J. 334 (2018) 768–779.
[83] F. Bi, Z. Zhao, Y. Yang, Q. Liu, W. Huang, Y. Huang, Efficient degradation of toluene over ultra-low Pd supported on UiO-66 and its functional materials: reaction mechanism, water-resistance, and influence of SO_2, Environ. Funct. Mater. 1 (2022) 166–181.
[84] Z. Lu, L. Guo, F. Bi, S. Ma, Q. Shen, R. Qiao, X. Zhang, Insight into the degradation mechanism of mixed VOCs oxidation over Pd/UiO-66(Ce) catalysts: combination of operando spectroscopy and theoretical calculation, Sep. Purif. Technol. 354 (2025) 129443.
[85] S.A. Abdul-wahab, F.A. Marikar, The environmental impact of gold mines: pollution by heavy metals, Cent. Eur. J. Eng. 2 (2012) 304–313.
[86] Y. Wei, W. Zhang, J. Gao, Trash or treasure? Sustainable noble metal recovery, Green. Chem. 26 (2024) 5684–5707.
[87] M. Sethurajan, E.D. Van Hullebusch, D. Fontana, A. Akcil, H. Deveci, B. Batinic, J. P. Leal, T.A. Gasche, M. Ali, K. Kuchta, I.F.F. Neto, H.M.V.M. Soares, H. Deveci, B. Batinic, J.P. Leal, T.A. Gasche, M.A. Kucuker, I.F.F. Neto, H.M.V.M. Soares, A. Chmielarz, Recent advances on hydrometallurgical recovery of critical and precious elements from end of life electronic wastes – a review, Crit. Rev. Environ. Sci. Technol. 49 (2019) 212–275.
[88] M. Wang, Q. Tan, J.F. Chiang, J. Li, Recovery of rare and precious metals from urban mines – a review, Front. Environ. Sci. Eng. 11 (2017) 1–17.
[89] U. Bardi, S. Caporali, U. Firenze, V.G. La Pira, D. Chimica, U. Firenze, V. Lastruccia, S. Fiorentino, Precious metals in automotive technology: an unsolvable depletion problem? Minerals 4 (2014) 388–398.
[90] X. Chen, E. Yu, S. Cai, E. Yu, H. Jia, S. Cai, P. Liang, J. Chen, J. Chen, In situ pyrolysis of Ce-MOF to prepare CeO_2 catalyst with obviously improved catalytic performance for toluene combustion, Chem. Eng. J. 344 (2018) 469–479.
[91] D.T. Wang, N. Guo, L.X. Jiang, S.Z. Lian, Z.W. Wang, Metal organic frameworks derived metal oxides prepared by oxygen vacancy engineering with the enhanced catalytic activity for toluene oxidation, J. Environ. Chem. Eng. 10 (2022) 108798.
[92] K. Li, C. Chen, H. Zhang, X. Hu, T. Sun, J. Jia, Effects of phase structure of MnO_2 and morphology of δ-MnO_2 on toluene catalytic oxidation, Appl. Surf. Sci. 496 (2019) 143662.
[93] Z. Feng, Q. Ren, R. Peng, S. Mo, M. Zhang, M. Fu, Effect of CeO_2 morphologies on toluene catalytic combustion, Catal. Today 332 (2019) 177–182.
[94] C. Zhang, W. Chu, F. Chen, L. Li, R. Jiang, J. Yan, Effects of cerium precursors on surface properties of mesoporous $CeMnO_x$ catalysts for toluene combustion, J. Rare Earths 38 (2020) 70–75.
[95] H. Sun, X. Yu, X. Ma, X. Yang, M. Lin, M. Ge, MnO_x-CeO_2 catalyst derived from metal-organic frameworks for toluene oxidation, Catal. Today 335 (2020) 580–586.
[96] L. Luo, R. Huang, W. Hu, Z. Yu, Z. Tang, L. Chen, Y. Zhang, D. Zhang, P. Xiao, Metal-organic framework-derived hollow $CoMn_2O_4$ nanocube catalysts for deep toluene oxidation, ACS Appl. Nano Mater. 5 (2022) 8232–8242.
[97] S. Qi, Y. Tao, S. Jiang, B. Chen, Z. Su, K. Chen, J. Wang, S. Luo, A. Xie, CeO_2 supported MOFs derived $LaB_xFe_yO_3$ (B=Mn, Co) perovskite catalysts for degradation of toluene, Environ. Sci. Pollut. Res. 30 (2023) 45414–45427.
[98] Z. Li, C. Ma, M. Qi, Y. Li, Y. Qu, Y. Zhang, L. Zhou, J. Yun, CeO_2 from pyrolysis of MOFs for efficient catalytic combustion of VOCs, Mol. Catal. 535 (2023) 112857.
[99] N. Sun, Y. Zhang, L. Wang, Z. Cao, J. Sun, Catalytic oxidation of toluene over Co-Cu bimetallic oxides derived from Co_yCu_{3-y}-MOF-74, J. Alloy. Compd. 928 (2022) 167105.
[100] X. Chen, S. Cai, E. Yu, H. Jia, X. Chen, X. Chen, S. Cai, E. Yu, J. Chen, H. Jia, J. Chen, J. Chen, MnO_x/Cr_2O_3 composites prepared by pyrolysis of Cr-MOF precursors containing in situ assembly of MnO_x as high stable catalyst for toluene oxidation, Appl. Surf. Sci. 475 (2019) 312–324.
[101] D. Leybo, U.J. Etim, M. Monai, S.R. Bare, Z. Zhong, C. Vogt, Metal-support interactions in metal oxide-supported atomic, cluster, and nanoparticle catalysis, Chem. Soc. Rev. 53 (2024) 10450–10490.
[102] J. Kim, D. Nam, H.J. Cho, E. Cho, D. Sivanesan, C. Cho, J. Lee, J. Kim, W. Choe, Up-down approach for expanding the chemical space of metal-organic frameworks, Nat. Synth. 3 (2024) 1518–1528.
[103] J. Chen, B. Bai, J. Lei, P. Wang, S. Wang, J. Li, Mn_3O_4 derived from Mn-MOFs with hydroxyl group ligands for efficient toluene catalytic oxidation, Chem. Eng. Sci. 263 (2022) 118065.
[104] W. Sun, X. Li, C. Sun, Z. Huang, H. Xu, W. Shen, Insights into the pyrolysis processes of Ce-MOFs for preparing highly active catalysts of toluene combustion, Catalysts 9 (2019) 682.
[105] X. Zhang, X. Lv, F. Bi, G. Lu, Y. Wang, Highly efficient Mn_2O_3 catalysts derived from Mn-MOFs for toluene oxidation: the influence of MOFs precursors, Mol. Catal. 482 (2020) 110701.
[106] J. Lei, S. Wang, J. Li, Mesoporous Co_3O_4 derived from facile calcination of octahedral Co-MOFs for toluene catalytic oxidation, Ind. Eng. Chem. Res. 59 (2020) 5583–5590.
[107] J. Lei, S. Wang, J. Li, Mesoporous Co_3O_4 derived from Co-MOFs with different morphologies and ligands for toluene catalytic oxidation, Chem. Eng. Sci. 220 (2020) 115654.
[108] J. Zhao, Z. Tang, F. Dong, J. Zhang, Controlled porous hollow Co_3O_4 polyhedral nanocages derived from metal-organic frameworks (MOFs) for toluene catalytic oxidation, Mol. Catal. 463 (2019) 77–86.
[109] X. Zhang, F. Bi, Z. Zhu, Y. Yang, S. Zhao, J. Chen, X. Lv, Y. Wang, J. Xu, N. Liu, The promoting effect of H_2O on rod-like $MnCeO_x$ derived from MOFs for toluene oxidation: a combined experimental and theoretical investigation, Appl. Catal. B Environ. 297 (2021) 120393.
[110] C. Dong, H. Wang, Y. Ren, Z. Qu, Effect of alkaline earth metal promoter on catalytic activity of MnO_2 for the complete oxidation of toluene, J. Environ. Sci. (China). 104 (2021) 102–112.
[111] Y. Zhang, Y. Li, Z. Zeng, J. Hu, Z. Huang, Promotion mechanism of $CuMn_2O_4$ modification with NaOH on toluene oxidation: boosting the ring-opening of benzoate, Fuel 314 (2022) 122747.
[112] X. Zhang, Z. Zhao, S. Zhao, S. Xiang, W. Gao, L. Wang, J. Xu, Y. Wang, The promoting effect of alkali metal and H_2O on Mn-MOF derivatives for toluene oxidation: a combined experimental and theoretical investigation, J. Catal. 415 (2022) 218–235.
[113] X. Yang, L. Chen, X. Yu, J. Yu, D. Han, M. Xiao, M. Ge, X. Yang, Exploration of atomic interfaces with inherent oxygen vacancies in zirconia for toluene oxidation, J. Mater. Chem. A 11 (2022) 287–296.
[114] X. Lai, X. Zhou, H. Zhang, X. Jiang, T. Lin, Y. Chen, Toluene oxidation over monolithic MnO_x/La-Al_2O_3 catalyst prepared by a CTAB-assisted impregnation method, Appl. Surf. Sci. 526 (2020) 146714.
[115] J. Lei, P. Wang, S. Wang, J. Li, Y. Xu, S. Li, Enhancement effect of Mn doping on Co_3O_4 derived from Co-MOF for toluene catalytic oxidation, Chin. J. Chem. Eng. 52 (2022) 1–9.
[116] D. Han, X. Ma, X. Yang, M. Xiao, H. Sun, L. Ma, X. Yu, M. Ge, Metal organic framework-templated fabrication of exposed surface defect-enriched Co_3O_4 catalysts for efficient toluene oxidation, J. Colloid Interface Sci. 603 (2021) 695–705.

[117] W. Li, G. Gao, L. Wang, H. Xu, W. Huang, N. Yan, Z. Qu, Dual confinement strategy based on metal-organic frameworks to synthesize MnO_x@ZrO_2 catalysts for toluene catalytic oxidation, Fuel 320 (2022) 123983.
[118] J. Zhao, P. Wang, C. Liu, Q. Zhao, J. Wang, L. Shi, G. Xu, A. Abudula, G. Guan, Nanosheet-state cobalt-manganese oxide with multifarious active regions derived from oxidation-etching of metal organic framework precursor for catalytic combustion of toluene, J. Colloid Interface Sci. 629 (2023) 706–722.
[119] Q. Ren, S. Mo, R. Peng, Z. Feng, M. Zhang, L. Chen, M. Fu, J. Wu, D. Ye, Controllable synthesis of 3D hierarchical Co_3O_4 nanocatalysts with various morphologies for the catalytic oxidation of toluene, J. Mater. Chem. A. 6 (2018) 498–509.
[120] F. Dong, W. Han, H. Zhao, G. Zhang, Z. Tang, Porous hollow $CoInO_x$ nanocubes as a highly efficient catalyst for the catalytic combustion of toluene, Nanoscale 11 (2019) 9937–9948.
[121] W. Han, F. Dong, W. Han, Z. Tang, Mn-polyacrylonitrile nanofibers decorated with Co-metal-organic frameworks as precursors of $CoMnO_x$ catalysts for the combustion of toluene, ACS Appl. Nano Mater. 3 (2020) 7818–7828.
[122] W. Han, H. Zhao, F. Dong, Z. Tang, Morphology-controlled synthesis of 3D, mesoporous, rosette-like $CeCoO_x$ catalysts by pyrolysis of $Ce[Co(CN)_6]$ and application for the catalytic combustion of toluene, Nanoscale 10 (2018) 21307–21319.
[123] D. Chen, J. Zhao, P. Zhang, S. Dai, Mechanochemical synthesis of metal–organic frameworks, Polyhedron 162 (2019) 59–64.
[124] W. Sun, Y. Huang, X. Li, Z. Huang, H. Xu, W. Shen, Catalytic combustion of toluene over highly dispersed Cu-CeO_x derived from Cu-Ce-MOF by EDTA grafting method, Catalysts 11 (2021) 519.
[125] J. Lei, S. Wang, J. Li, Y. Xu, S. Li, Different effect of Y (Y = Cu, Mn, Fe, Ni) doping on Co_3O_4 derived from Co-MOF for toluene catalytic destruction, Chem. Eng. Sci. 251 (2022) 117436.
[126] A. Yusuf, C. Snape, J. He, H. Xu, C. Liu, M. Zhao, G.Z. Chen, B. Tang, C. Wang, J. Wang, N. Sailesh, A. Yusuf, C. Snape, J. He, H. Xu, C. Liu, M. Zhao, Advances on transition metal oxides catalysts for formaldehyde oxidation: a review, Catal. Rev. 59 (2017) 189–233.
[127] J. Eun, Y. Sik, D.C.W. Tsang, J. Song, S. Jung, Y. Park, Recent advances in volatile organic compounds abatement by catalysis and catalytic hybrid processes: a critical review, Sci. Total Environ. 719 (2020) 137405.
[128] J.W.M. Osterrieth, D. Wright, H. Noh, C.W. Kung, D. Vulpe, A. Li, J.E. Park, R. P. Van Duyne, P.Z. Moghadam, J.J. Baumberg, O.K. Farha, D. Fairen-Jimenez, Core-shell gold nanorod@Zirconium-based metal-organic framework composites as in situ size-selective Raman probes, J. Am. Chem. Soc. 141 (2019) 3893–3900.
[129] H. Li, F. Yue, H. Xie, C. Yang, Y. Zhang, L. Zhang, J. Wang, Hollow shell-in-shell Ni_3S_4@Co_9S_8 tubes derived from core-shell Ni-MOF-74@Co-MOF-74 as efficient faradaic electrodes, CrystEngComm 20 (2018) 889–895.
[130] T. Bogaerts, V.Y.D.D. Andy, Y.Y. Liu, F. Lynen, V. Van Speybroeck, V.D.V. Pascal, Mn-salen@MIL101(Al): a heterogeneous, enantioselective catalyst synthesized using a 'bottle around the ship' approach, Chem. Commun. 49 (2013) 8021–8023.
[131] X. Gu, C. Huang, Z. Xu, H. Wu, R. Dong, R. Liu, J. Chen, H. Zhu, Core-shell Co-MOF-74@Mn-MOF-74 catalysts with controllable shell thickness and their enhanced catalytic activity for toluene oxidation, J. Solid State Chem. 294 (2021) 121803.
[132] C. Dong, Z. Qu, Y. Qin, Q. Fu, H. Sun, X. Duan, Revealing the highly catalytic performance of spinel $CoMn_2O_4$ for toluene oxidation: involvement and replenishment of oxygen species using in Situ designed-TP techniques, ACS Catal. 9 (2019) 6698–6710.
[133] J. Zhao, W. Han, J. Zhang, Z. Tang, In situ growth of Co_3O_4 nano-dodecahedeons on In_2O_3 hexagonal prisms for toluene catalytic combustion, Arab. J. Chem. 13 (2020) 4857–4867.
[134] Y. Li, W. Han, R. Wang, L.T. Weng, A. Serrano-Lotina, M.A. Bañares, Q. Wang, K. L. Yeung, Performance of an aliovalent-substituted $CoCeO_x$ catalyst from bimetallic MOF for VOC oxidation in air, Appl. Catal. B Environ. 275 (2020) 119121.
[135] A. Gupta, U.V. Waghmare, M.S. Hegde, Correlation of oxygen storage capacity and structural distortion in transition-metal-, noble-metal-, and rare-earth-ion-substituted CeO_2 from first principles calculation, Chem. Mater. 22 (2010) 5184–5198.
[136] M. Wang, F. Li, J. Dong, X. Lin, X. Liu, D. Wang, W. Cai, MOF-derived $CoCeO_x$ nanocomposite catalyst with enhanced anti-coking property for ethanol reforming with CO_2, J. Environ. Chem. Eng. 10 (2022) 107892.
[137] X. Weng, P. Sun, Y. Long, Q. Meng, Z. Wu, Catalytic oxidation of chlorobenzene over $Mn_xCe_{1-x}O_2$/HZSM-5 catalysts: a study with practical implications, Environ. Sci. Technol. 51 (2017) 8057–8066.
[138] H. Sun, X. Yu, X. Ma, X. Yang, M. Lin, M. Ge, MnO_x-CeO_2 catalyst derived from metal-organic frameworks for toluene oxidation, Catal. Today 355 (2020) 580–586.
[139] T. Chen, R. Wang, C. Sun, D. Kong, S. Lu, X. Li, Metal-organic frameworks templated micropore-enriched defective $MnCeO_x$ for low temperature chlorobenzene oxidation, Appl. Catal. A Gen. 645 (2022) 118845.
[140] B. Chen, X. Yang, X. Zeng, Z. Huang, J. Xiao, J. Wang, G. Zhan, Multicomponent metal oxides derived from Mn-BTC anchoring with metal acetylacetonate complexes as excellent catalysts for VOCs and CO oxidation, Chem. Eng. J. 397 (2020) 125424.
[141] Y. Guo, M. Wen, S. Song, Q. Liu, G. Li, T. An, Enhanced catalytic elimination of typical VOCs over $ZnCoO_x$ catalyst derived from in situ pyrolysis of ZnCo bimetallic zeolitic imidazolate frameworks, Appl. Catal. B Environ. 308 (2022) 121212.
[142] P. Wang, J. Wang, J. Shi, X. Du, X. Hao, B. Tang, A. Abudula, G. Guan, Low content of samarium doped CeO_2 oxide catalysts derived from metal organic framework precursor for toluene oxidation, Mol. Catal. 492 (2020) 111027.
[143] M. Lammert, M.T. Wharmby, S. Smolders, B. Bueken, A. Lieb, K.A. Lomachenko, D.De Vos, N. Stock, Cerium-based metal organic frameworks with UiO-66 architecture: synthesis, properties and redox catalytic activity, Chem. Commun. 51 (2015) 12578–12581.
[144] X. Hou, Y. Bian, L. Yang, One-step synthesis of transition metal modified UiO-66-Ce metal-organic framework: catalytic oxidation of toluene and investigation of the mechanism, Microporous Mesoporous Mater. 345 (2022) 112214.
[145] W. Zhang, X. Jiang, Y. Zhao, A. Carné-Sánchez, V. Malgras, J. Kim, J.H. Kim, S. Wang, J. Liu, J. Sen Jiang, Y. Yamauchi, M. Hu, Hollow carbon nanobubbles: monocrystalline MOF nanobubbles and their pyrolysis, Chem. Sci. 8 (2017) 3538–3546.
[146] X. Zhang, S. Xiang, Q. Du, F. Bi, K. Xie, L. Wang, Effect of calcination temperature on the structure and performance of rod-like $MnCeO_x$ derived from MOFs catalysts, Mol. Catal. 522 (2022) 112226.
[147] R. Zhao, X. Zhao, Z. Liu, F. Ding, Z. Liu, Controlling the orientations of h-BN during growth on transition metals by chemical vapor deposition, Nanoscale 9 (2017) 3561–3567.
[148] N.M. Padial, B. Lerma-Berlanga, N. Almora-Barrios, J. Castells-Gil, I. Da Silva, M. De La Mata, S.I. Molina, J. Hernández-Saz, A.E. Platero-Prats, S. Tatay, C. MartÍ-Gastaldo, Heterometallic titanium-organic frameworks by metal-induced dynamic topological transformations, J. Am. Chem. Soc. 142 (2020) 6638–6648.
[149] Q. Wang, Z. Li, M.A. Banares, L.-T. Weng, Q. Gu, J. Price, W. Han, K.L. Yeung, A novel approach to high-performance aliovalent-substituted catalysts 2D bimetallic MOF-derived CeCuOx microsheets, Small 15 (2019) 1903525.
[150] J. Zhao, Z. Tang, F. Dong, J. Zhang, Controlled porous hollow Co_3O_4 polyhedral nanocages derived from metal-organic frameworks (MOFs) for toluene catalytic oxidation, Mol. Catal. 463 (2019) 77–86.
[151] H. Wang, M. Liu, S. Guo, Y. Wang, X. Han, Y. Bai, Efficient oxidation of o-xylene over CeO_2 catalyst prepared from a Ce-MOF template: the promotion of K^+ embedding substitution, Mol. Catal. 436 (2017) 120–127.
[152] J. Mei, Y. Shen, Q. Wang, Y. Shen, W. Li, J. Zhao, J. Chen, S. Zhang, Roles of oxygen species in low-temperature catalytic o-xylene oxidation on MOF-derived bouquetlike CeO_2, ACS Appl. Mater. Interfaces 14 (2022) 35694–35703.
[153] X. Zhang, X. Lv, F. Bi, G. Lu, Y. Wang, Highly efficient Mn_2O_3 catalysts derived from Mn-MOFs for toluene oxidation: the influence of MOFs precursors, Mol. Catal. 482 (2020) 110701.
[154] W. Sun, X. Li, C. Sun, Z. Huang, H. Xu, W. Shen, Insights into the pyrolysis processes of Ce-MOFs for preparing highly active catalysts of toluene combustion, Catalysts 9 (2019) 682.
[155] J. Mei, S. Zhang, G. Pan, Z. Cheng, J. Chen, J. Zhao, Surfactant-assisted synthesis of MOF-derived CeO_2 for low-temperature catalytic o-xylene combustion, J. Environ. Chem. Eng. 10 (2022) 108743.
[156] X. Chen, X. Chen, E. Yu, S. Cai, H. Jia, J. Chen, P. Liang, In situ pyrolysis of Ce-MOF to prepare CeO_2 catalyst with obviously improved catalytic performance for toluene combustion, Chem. Eng. J. 344 (2018) 469–479.
[157] X. Ma, W. Wang, X. Zhang, H. Li, J. Sun, X. Liu, C. Sun, MOF-derived FeO_x with highly dispersed active sites as an efficient catalyst for enchaning catalytic oxidation of VOCs, J. Environ. Chem. Eng. 12 (2024) 111966.
[158] J.R. Li, F.K. Wang, C. He, C. Huang, H. Xiao, Catalytic total oxidation of toluene over carbon-supported Cu-Co oxide catalysts derived from Cu-based metal organic framework, Powder Technol. 363 (2020) 95–106.
[159] Q. Zhang, Y. Jiang, J. Gao, M. Fu, S. Zou, Y. Li, Interfaces in MOF-derived CeO_2-MnO_x composites as high-activity catalysts for toluene oxidation: Monolayer dispersion threshold, Catalysts 10 (2020) 1–15.
[160] Y. Li, W. Han, R. Wang, L.T. Weng, A. Serrano-Lotina, M.A. Bañares, Q. Wang, K. L. Yeung, Performance of an aliovalent-substituted $CoCeO_x$ catalyst from bimetallic MOF for VOC oxidation in air, Appl. Catal. B Environ. 275 (2020) 119121.
[161] H. Sun, X. Yu, X. Ma, X. Yang, M. Lin, M. Ge, MnO_x-CeO_2 catalyst derived from metal-organic frameworks for toluene oxidation, Catal. Today 355 (2020) 580–586.
[162] Q. Wang, Z. Li, M.A. Bañares, L.T. Weng, Q. Gu, J. Price, W. Han, K.L. Yeung, A novel approach to high-performance aliovalent-substituted catalysts—2D bimetallic MOF-derived $CeCuO_x$ microsheets, Small 15 (2019) 1–7.
[163] W. Hu, J. Huang, J. Xu, S. Cheng, Y. Lyu, D. Xie, Z. Wang, Insights into the superior performance of mesoporous MOFs-derived Cu–Mn oxides for toluene total catalytic oxidation, Fuel Process. Technol. 236 (2022) 107424.
[164] Q. Huang, P. Zhao, W. Wang, L. Lv, W. Zhang, B. Pan, In situ fabrication of highly dispersed Co-Fe-doped-δ-MnO_2 catalyst by a facile redox driving MOFs-derived method for low temperature oxidation of toluene, 14 (2022) 53872–53883.
[165] Y. Shan, N. Gao, Y. Chen, S. Shen, Self-template synthesis of a $MnCeO_δ$/Co_3O_4 polyhedral nanocage catalyst for toluene oxidation, Ind. Eng. Chem. Res. 58 (2019) 16370–16378.
[166] F. Dong, W. Han, Y. Guo, W. Han, Z. Tang, $CeCoO_x$-MNS catalyst derived from three-dimensional mesh nanosheet Co-based metal–organic frameworks for highly efficient catalytic combustion of VOCs, Chem. Eng. J. 405 (2021) 126948.
[167] L. Lv, Z. Zhang, S. Wang, Y. Shan, Y. Chen, T. Wei, Catalytic oxidation of toluene over Co_3O_4-CeO_2 bimetal oxides derived from Ce-based MOF, Mol. Catal. 551 (2023) 113645.
[168] N. Wu, C. Zhang, J. Li, Y. Shi, Q. Wang, S. Wu, S. Yao, Z. Wu, E. Gao, W. Wang, J. Zhu, L. Li, In situ synthesis of MOF-derived $CuCoO_x$ with enhanced catalytic activity and moisture resistance for aromatic VOCs combustion: the role of

bimetallic oxide interactions on the catalytic mechanism, Sep. Purif. Technol. 341 (2024) 126947.
[169] Y. Wang, Z. Chen, S. Lu, S. Xin, G. Liu, C. Zhou, Y. Xin, Q. Wang, Q. Wang, Y. Wang, T. Xue, Q. Yan, Efficient oxidation and stable removal of toluene over controlled metal-organic framework derived $MnFeO_x$ catalysts, Mol. Catal. 553 (2024) 113792.
[170] B. Ahmad, A. Ismail, Y. Li, Z. Sun, Y. Zhu, Excellent low-temperature catalytic performance on toluene oxidation over spinel $Ce_aMn_{3-a}O_4$ catalyst derived from pyrolysis of metal organic framework, Sep. Purif. Technol. 360 (2025) 131130.
[171] N. Tang, Z. You, M. Li, S. Jiang, Y. He, Promotion of toluene catalytic oxidation by M−La/CoO_x catalysts directly prepared from Co-MOFs precursors, Sep. Purif. Technol. 349 (2024) 127754.
[172] R. Yu, Q. Jiao, J. Zhu, L. Li, M. Huang, C. Fang, Porous $LaMO_3$ (M = Co, Mn, Fe) perovskite oxides derived from MOFs as efficient catalysts for toluene oxidation, J. Alloy. Compd. 1013 (2025) 178617.
[173] X. Jin, Z. Zhang, Y. Zhu, X. Jin, D. Liu, S. Hou, Q. Ge, Z. Zhao, Z. Zhang, $CeCo_aO_x$ catalysts derived from metal-organic frameworks for enhancing catalytic toluene oxidation by tuning surface oxygen property, Appl. Surf. Sci. 672 (2024) 160841.
[174] N. Wu, C. Zhang, J. Li, Y. Shi, Q. Wang, S. Wu, S. Yao, Z. Wu, E. Gao, W. Wang, J. Zhu, L. Li, In situ synthesis of MOF-derived $CuCoO_x$ with enhanced catalytic activity and moisture resistance for aromatic VOCs combustion: the role of bimetallic oxide interactions on the catalytic mechanism, Sep. Purif. Technol. 341 (2024) 126947.
[175] Jinbo Wang, B. Xia, R. Qin, S. Zhao, Y. Qiu, J. Li, Y. Wang, Highly stable MOFs-derived Cu–Co composite metal oxides for catalytic oxidation of toluene, Russ. J. Phys. Chem. A 98 (2024) 1713–1720.
[176] B. Gao, F. Bi, Z. Zhou, Y. Zhang, J. Wei, X. Lv, B. Liu, Y. Huang, X. Zhang, A bimetallic MOF-derived MnCo spinel oxide catalyst to enhance toluene catalytic degradation, Chem. Commun. 60 (2024) 7455–7458.
[177] F. Zhang, H. Zhang, D. Wu, Performance of an aliovalent-doping $MnCeO_x$/cordierite monolithic catalyst derived from MOFs for o-Xylene oxidation, Catal. Lett. 154 (2024) 1893–1906.
[178] P. Wang, J. Wang, X. An, J. Shi, W. Shangguan, X. Hao, G. Xu, B. Tang, A. Abudula, G. Guan, Generation of abundant defects in Mn-Co mixed oxides by a facile agar-gel method for highly efficient catalysis of total toluene oxidation, Appl. Catal. B Environ. 282 (2021) 119560.
[179] Q. Huang, P. Zhao, W. Wang, L. Lv, W. Zhang, B. Pan, In situ Fabrication of highly dispersed Co-Fe-doped-δ-MnO_2 catalyst by a facile redox-driving MOFs-derived method for low-temperature oxidation of toluene, ACS Appl. Mater. Interfaces 14 (2022) 53872–53883.
[180] Y. Wang, J. Wu, G. Wang, D. Yang, T. Ishihara, L. Guo, Oxygen vacancy engineering in Fe doped akhtenskite-type MnO_2 for low-temperature toluene oxidation, Appl. Catal. B Environ. 285 (2021) 119873.
[181] Z. Su, W. Yang, C. Wang, S. Xiong, X. Cao, Y. Peng, W. Si, Y. Weng, M. Xue, J. Li, Roles of oxygen vacancies in the bulk and surface of CeO_2 for toluene catalytic combustion, Environ. Sci. Technol. 54 (2020) 12684–12692.
[182] Y. Wang, X. Li, J. Xiao, D. Chen, N. Li, Q. Xu, H. Li, J. He, J. Lu, Metal-organic frameworks-derived manganese trioxide with uniformly loaded ultrasmall platinum nanoparticles boosting benzene combustion, Sci. Total Environ. 839 (2022) 156345.
[183] P. Brandt, S.H. Xing, J. Liang, G. Kurt, A. Nuhnen, O. Weingart, C. Janiak, Zirconium and aluminum MOFs for low-pressure SO_2 adsorption and potential separation: elucidating the effect of small pores and NH_2 groups, ACS Appl. Mater. Interfaces 13 (2021) 29137–29149.
[184] Z. Li, F. Liao, F. Jiang, B. Liu, S. Ban, G. Chen, C. Sun, P. Xiao, Y. Sun, Capture of H_2S and SO_2 from trace sulfur containing gas mixture by functionalized UiO-66 (Zr) materials: a molecular simulation study, Fluid Phase Equilib. 427 (2016) 259–267.
[185] D. Zhang, X. Jing, D.S. Sholl, S.B. Sinnott, Molecular simulation of capture of sulfur-containing gases by porous aromatic frameworks, J. Phys. Chem. C 122 (2018) 18456–18467.
[186] Y. Zheng, K. Fu, Z. Yu, Y. Su, R. Han, Q. Liu, Oxygen vacancies in a catalyst for VOCs oxidation: synthesis, characterization, and catalytic effects, J. Mater. Chem. A 10 (2022) 14171–14186.
[187] M. Shahzad, S.A. Razzak, M.M. Hossain, Catalytic oxidation of volatile organic compounds (VOCs) – a review, Atmos. Environ. 140 (2016) 117–134.
[188] K. Zhang, H. Ding, W. Pan, X. Mu, K. Qiu, J. Ma, Y. Zhao, J. Song, Research progress of a composite metal oxide catalyst for VOC degradation, Environ. Sci. Technol. 56 (2022) 9220–9236.